

SFU

SIMON FRASER UNIVERSITY
ENGAGING THE WORLD

Deep learning for skin image analysis

Beyond more data and faster GPUs

Ghassan Hamarneh

hamarneh@sfu.ca

www.MedicalImageAnalysis.com

17 June 2019

ISIC Skin Image Analysis Workshop at CVPR

Acknowledgements

Current and former students



Dr. Jeremy Kawahara



Dr. Hengameh Mirzaalian



Dr. Aicha Bentaieb



Saeid Asgari



Zahra MiriKharaji



Saeed Izadi



Yiqi Yan



Kumar Abhishek



Chris Yoon

Funding: research, infrastructure, computing



Disclosure

Scientific Advisor and Shareholder:
Triage Technologies Inc.

Skin image analysis system

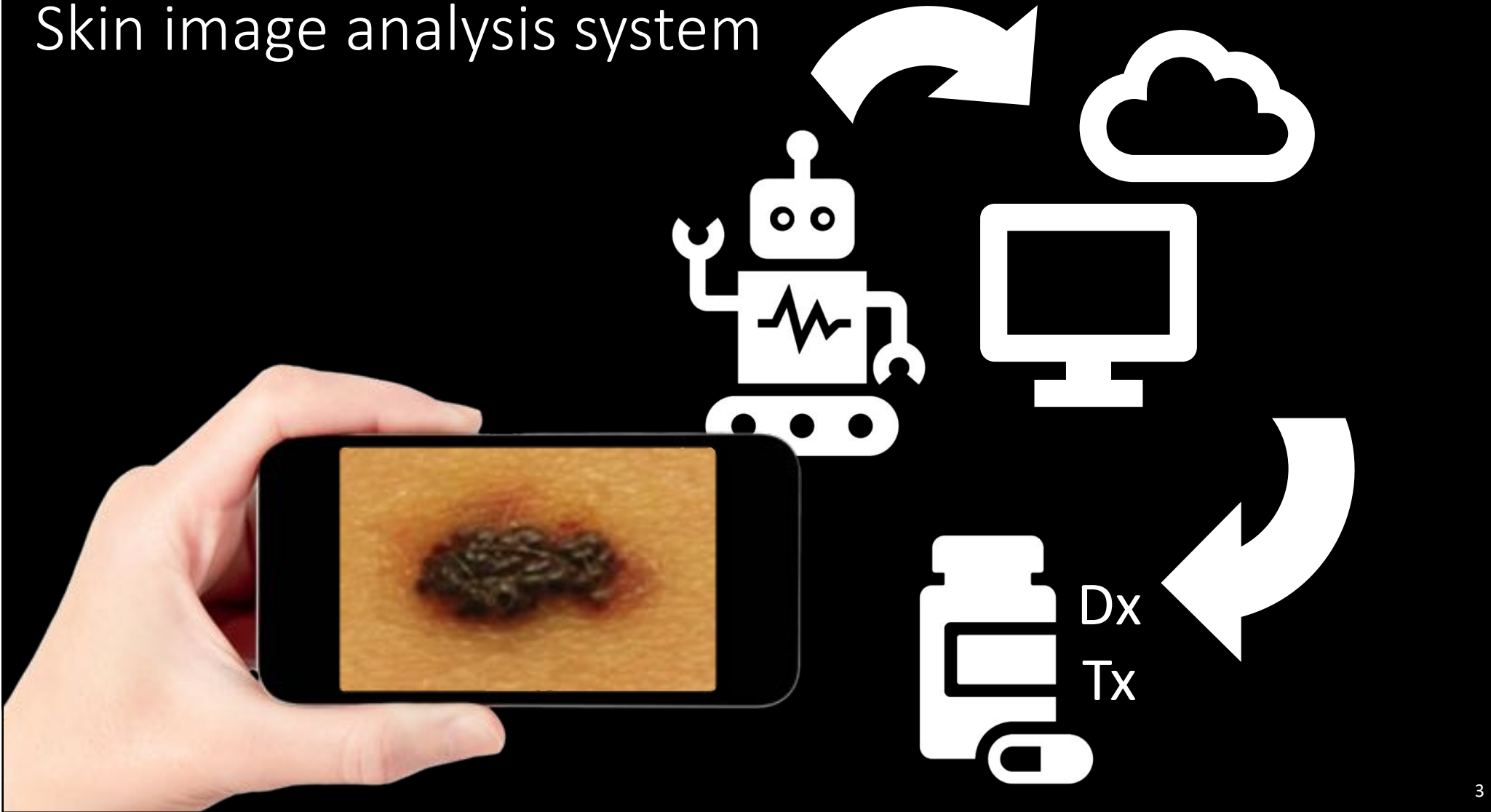
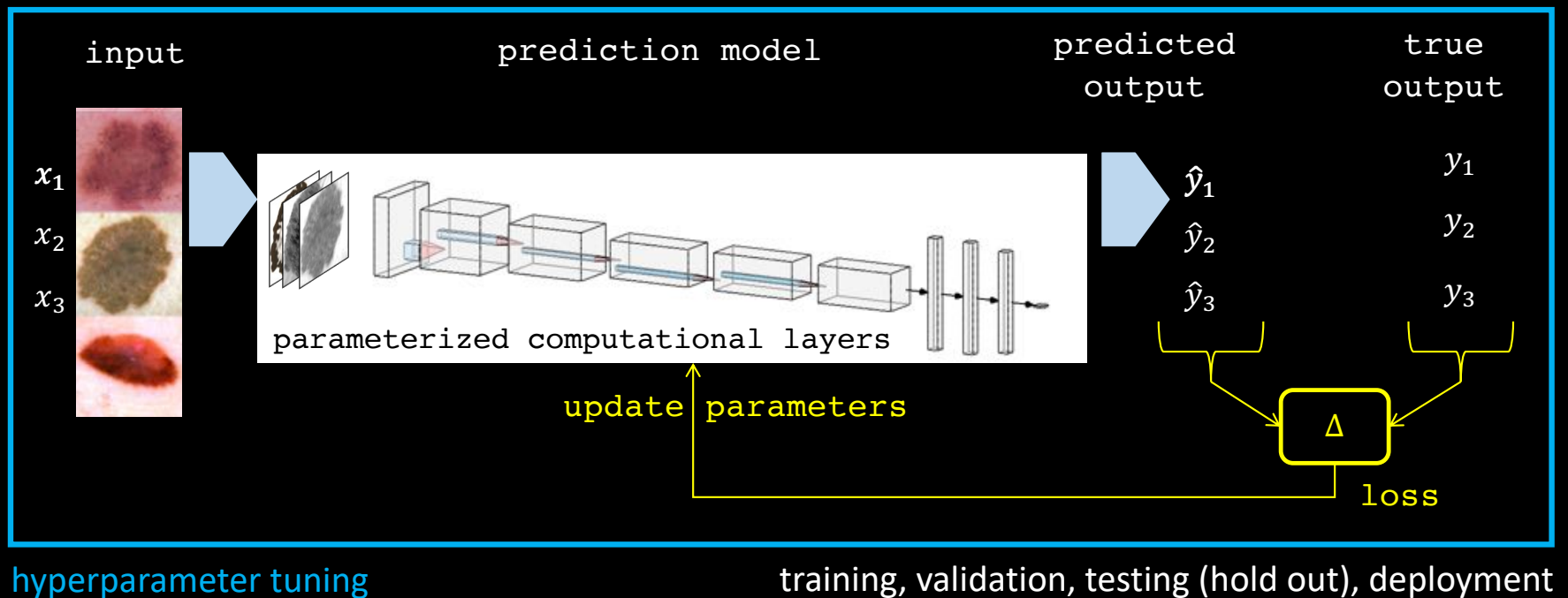
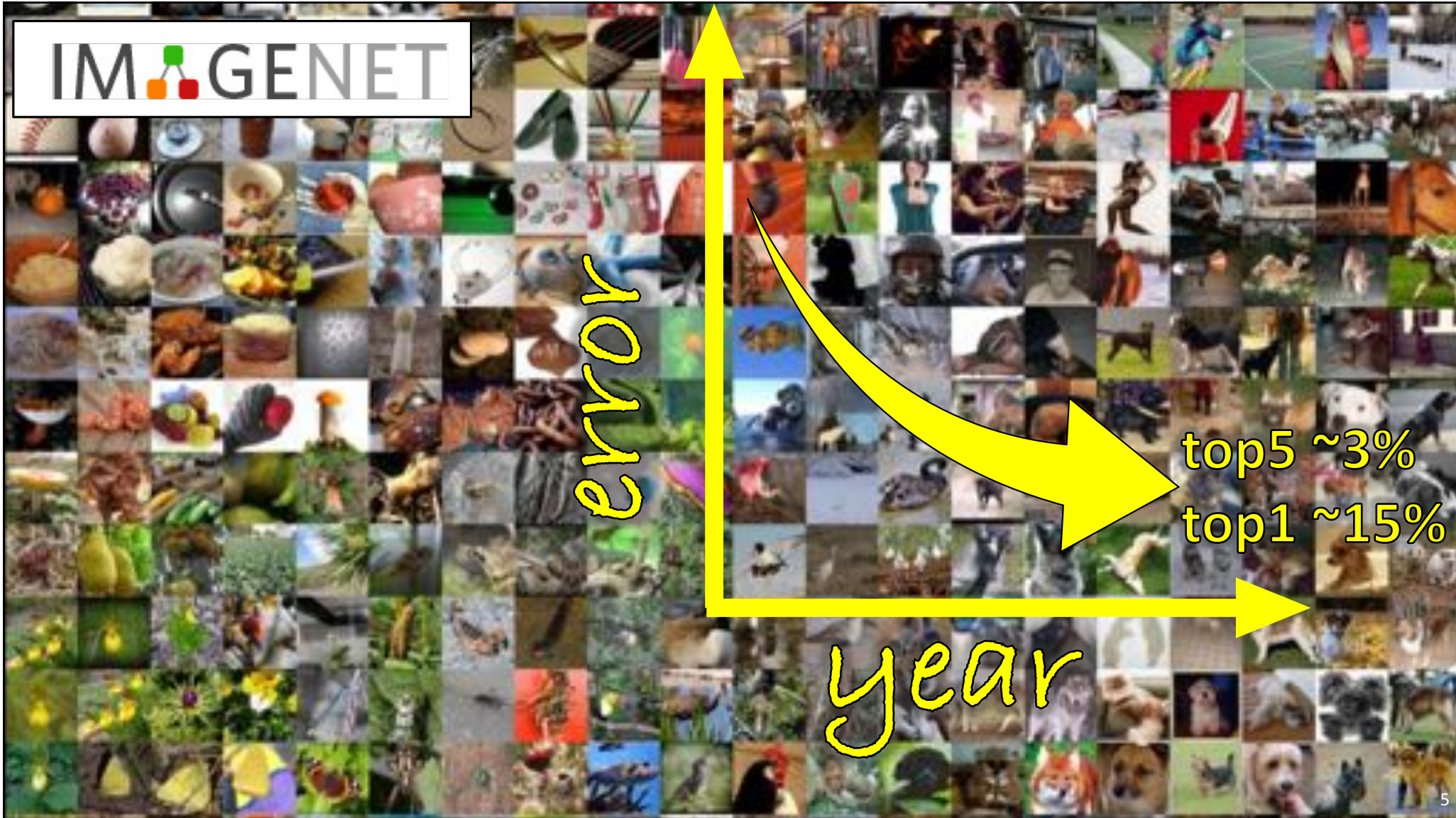
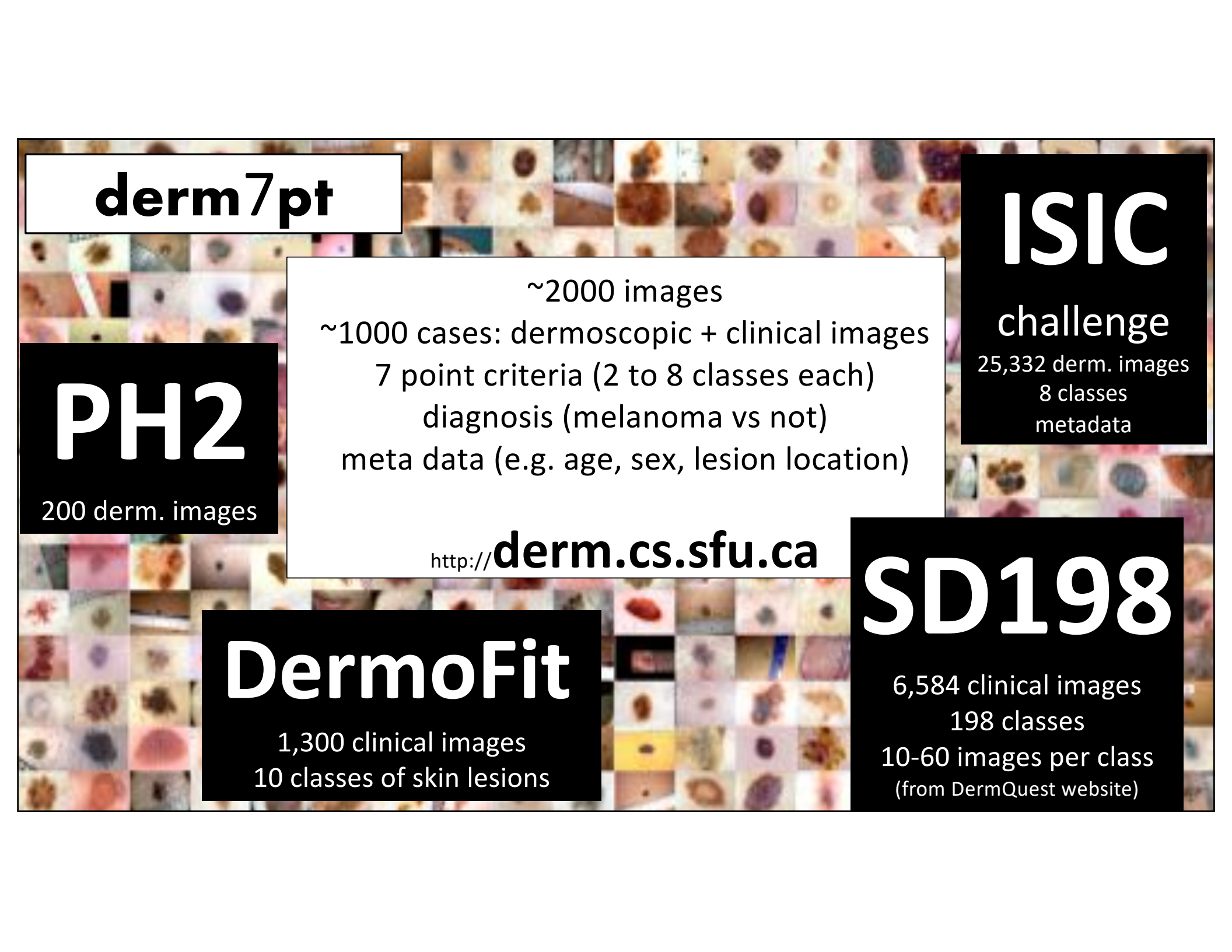


Image analysis via deep learning



IMAGENET





derm7pt

PH2

200 derm. images

DermoFit

1,300 clinical images
10 classes of skin lesions

~2000 images

~1000 cases: dermoscopic + clinical images

7 point criteria (2 to 8 classes each)

diagnosis (melanoma vs not)

meta data (e.g. age, sex, lesion location)

<http://derm.cs.sfu.ca>

ISIC challenge

25,332 derm. images
8 classes
metadata

SD198

6,584 clinical images
198 classes
10-60 images per class
(from DermQuest website)

nature
International Journal of science

Letter | Published: 25 January 2017

Jan. 2017

Dermatologist-level classification of skin cancer with deep neural networks

Andre Esteva , Brett Kuprel , Roberto A. Novoa , Justin Ko, Susan M. Swetter, Helen M. Blau & Sebastian Thrun 

Nature 542, 115–118 (02 February 2017) | Download Citation 

<https://www.nature.com/articles/nature21056>

ANNALS OF ONCOLOGY

"CNN ROC AUC greater than mean ROC area of dermatologists... higher specificity"

Man against machine: diagnostic performance of a deep learning convolutional neural network for dermoscopic melanoma recognition in comparison to 58 dermatologists

H. A. Haenssle^{1,*†}, C. Fink^{1†}, R. Schneiderbauer¹, F. Toberer¹, T. Buhl², A. Blum³, A. Kalloo⁴, A. Ben Hadj Hassen⁵, L. Thomas⁶, A. Enk¹ & L. Uhlmann⁷

August 2018

<https://academic.oup.com/annonc/article/29/8/1836/5004443>

GENERAL DERMATOLOGY

Feb. 2019

BJD
British Journal of Dermatology

Deep-learning-based, computer-aided classifier developed with a small dataset of clinical images **surpasses** board-certified dermatologists in skin tumour diagnosis*

Y. Fujisawa , Y. Otomo, Y. Ogata, Y. Nakamura, R. Fujita, Y. Ishitsuka, R. Watanabe, N. Okiyama , K. Ohara⁴ and M. Fujimoto¹

<https://onlinelibrary.wiley.com/doi/abs/10.1111/bjd.17470>

EJC
EUROPEAN JOURNAL OF CANCER

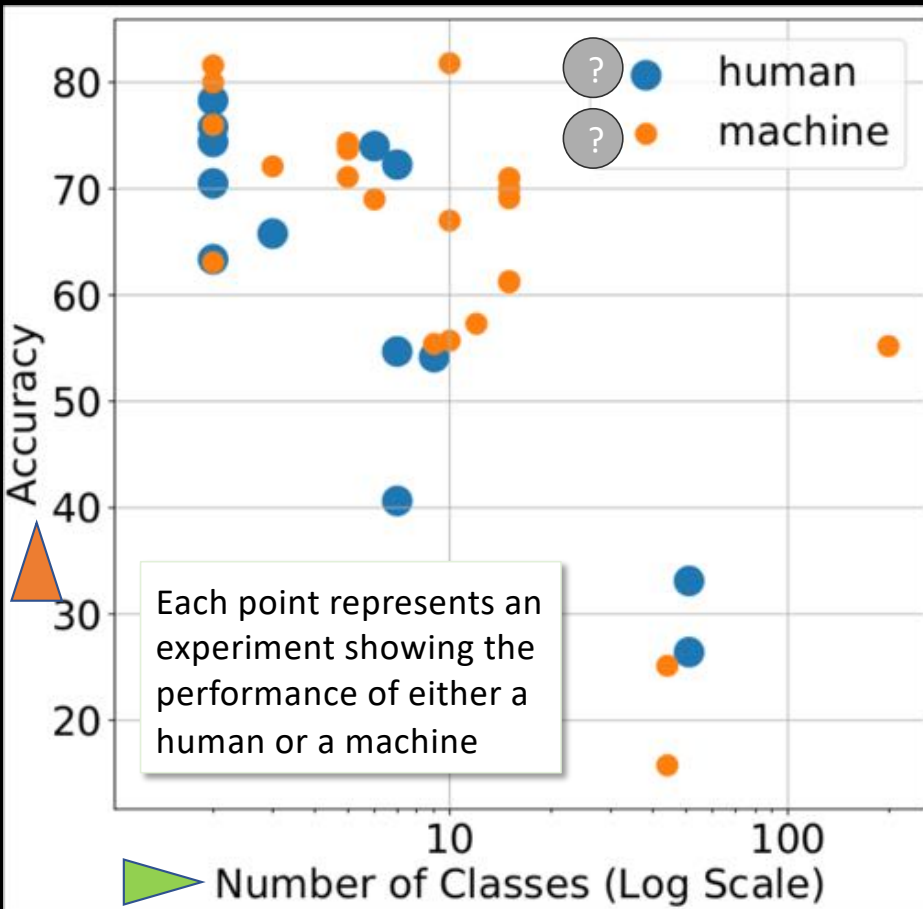
May 2019

Deep learning **outperformed** 136 of 157 dermatologists in a head-to-head dermoscopic melanoma image classification task

Titus J. Brinker ^{a,b,*}, Achim Hekler ^a, Alexander H. Enk ^b, Joachim Klode ^c, Axel Hauschild ^d, Carola Berking ^e, Bastian Schilling ^f, Sebastian Haferkamp ^g, Dirk Schadendorf ^c, Tim Holland-Letz ^h, Jochen S. Utikal ^{i,j,l}, Christof von Kalle ^{a,l}, Collaborators²

<https://www.sciencedirect.com/science/article/pii/S0959804919302217>

human vs machine



arXiv.org > cs > arXiv:1906.01256

Computer Science > Computer Vision and Pattern Recognition

Visual Diagnosis of Dermatological Disorders: Human and Machine Performance

June 2019

<https://arxiv.org/abs/1906.01256>

Jeremy Kawahara, Ghassan Hamarneh

Year	Dataset	N.Images	N.Test	Derm. Clinic.	Meta	H.vs.M	Classes	Acc.
[89]	2015	Internal	-	65	✓	human	2	63.35
[89]	2015	Internal	273	65	✓	machine	2	63.08
[90]	2017	ISIC-100	-	100	✓	human	2	70.50
[90]	2017	ISIC-100	1000	100	✓	machine	2	76.00
[96]	2018	Internal	-	100	✓	human	2	74.40
[96]	2018	Internal	-	100	✓	✓ human	2	78.30
[96]	2018	Internal	-	100	✓	machine	2	81.60
[94]	2018	Asan	-	1133	✓	human	2	75.80
[94]	2018	Asan	49,567	1133	✓	machine	2	80.00
[97]	2019	ISIC-100	13737	100	✓	machine	2	84.02
[39]	2019	ISIC-100	-	100	✓	human	2	62.82
[39]	2019	MED-NODE	-	100	✓	human	2	69.40
[41]	2017	Stanford	-	180	✓	✓ human	3	65.78
[41]	2017	Stanford	127,463	127,463	✓	✓ machine	3	72.10
[22]	2013	Dermofit	960	960	✓	machine	5	74.30
[83]	2018	Atlas	2018	395	✓	✓ machine	5	71.10
[83]	2018	Atlas	2018	395	✓	✓ machine	5	73.70
[93]	2017	Internal	348	50	✓	human	6	74.00
[93]	2017	Internal	348	50	✓	✓ machine	6	69.00
[102]	2002	Internal	-	256	✓*	✓ human	7	40.62
[102]	2002	Internal	-	256	✓	✓ human	7	54.69
[102]	2002	Internal	-	256	✓*	✓ human	7	72.27
[43]	2017	Stanford	-	180	✓	✓ human	9	54.15
[43]	2017	Stanford	127,463	127,463	✓	✓ machine	9	55.40
[57]	2015	Dermofit	1300	1300	✓	✓ machine	10	67.00
[66]	2016	Dermofit	1300	1300	✓	✓ machine	10	81.80
[42]	2018	Dermofit	20,689	1300	✓	✓ machine	10	55.70
[42]	2018	Asan	19,389	1,276	✓	✓ machine	12	57.30
[98]	2019	Internal	-	1260	✓	human	14	41.70
[98]	2019	Internal	-	1820	✓	human	14	59.70
[98]	2019	Internal	6009	1142	✓	✓ machine	14	76.50
[45]	2017	MoleMap	40,373	1776	✓	✓ machine	15	69.10
[80]	2017	MoleMap	205,842	2975	✓	✓ machine	15	61.20
[80]	2017	MoleMap	205,842	3475	✓	✓ machine	15	61.30
[80]	2017	MoleMap	205,842	3975	✓	✓ machine	15	70.00
[77]	2017	MoleMap	32,395	8,012	✓	✓ machine	15	73.00
[32]	2014	dermos	2309	1,429	✓	✓ machine	44	15.76
[32]	2014	dermos	2309	1,429	✓	✓ machine	44	25.12
[100]	2017	Internal	-	272	✓	✓ machine	51	37.77
[100]	2017	Internal	-	2072	✓	human	51	35.10
[132]	2016	SDC-398	6,584	3292	✓	✓ machine	108	52.19
[776]	2018	Skin-1000	-	-	✓	human	108	59.00
[763]	2018	Skin-1000	-	-	✓	human	108	59.00
[773]	2018	Skin-1000	-	-	✓	human	108	59.00

Skin conditions

**1029 skin conditions
excluding melanoma, neoplasms**

ICD-10 Version:2016

- ▼ XII Diseases of the skin and subcutaneous tissue
 - ▶ L00-L08 Infections of the skin and subcutaneous tissue
 - ▶ L10-L14 Bullous disorders
 - ▶ L20-L30 Dermatitis and eczema
 - ▶ L40-L45 Papulosquamous disorders
 - ▶ L50-L54 Urticaria and erythema
 - ▶ L55-L59 Radiation-related disorders of the skin and subcutaneous tissue
 - ▶ L60-L75 Disorders of skin appendages
 - ▶ L80-L99 Other disorders of the skin and subcutaneous tissue

<https://icd.who.int/browse10/2016/en>

- ▼ D03 Melanoma in situ
- ▼ D04 Carcinoma in situ of skin
- ▼ D23 Other benign neoplasms of skin
- ▼ C43-C44 Melanoma and other malignant neoplasms of skin

Which classes to predict?

Large number of hierarchical conditions

Which conditions, at what level of granularity?

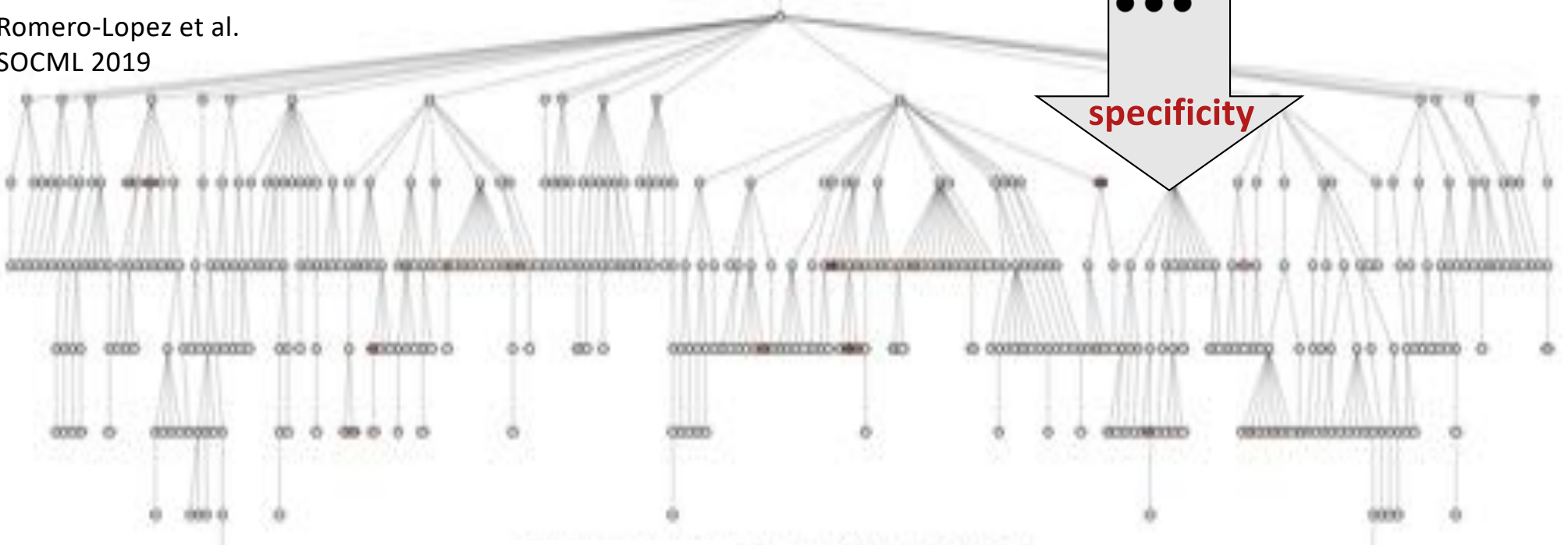
max specificity f
subject to:
 $\text{accuracy } (f) \geq 1 - \epsilon$

accuracy

specificity

Deng, Krause, Berg, Fei-Fei
CVPR 2012 
<https://ieeexplore.ieee.org/document/6248086>

Romero-Lopez et al.
SOCML 2019

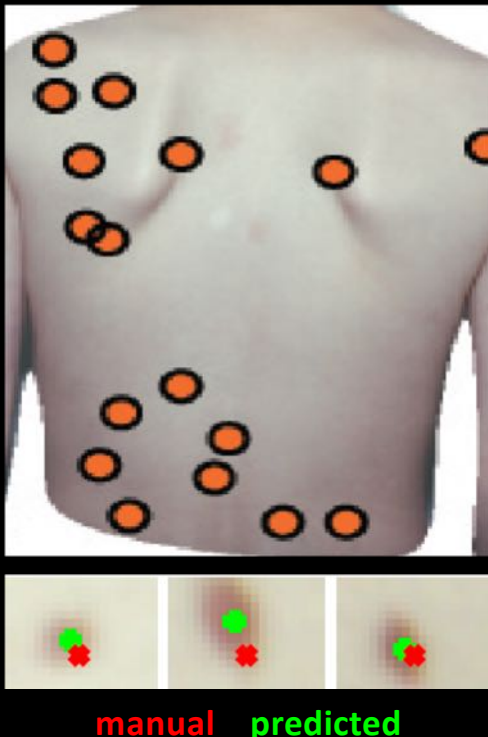


skin conditions ontology

133 diagnosis nodes parents to 588 different skin conditions

Other prediction tasks

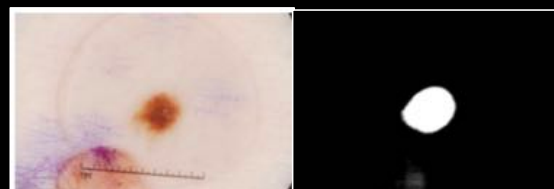
localize



Mirzaalian, Hamarneh, Lee
CVPR 2009

<https://doi.ieeecomputersociety.org/10.1109/CVPR.2009.5206725>

segment

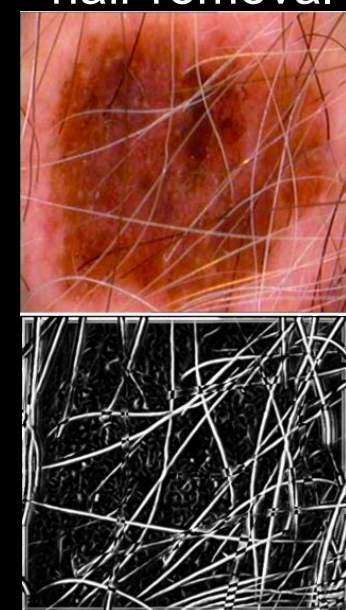


Mirikhariji, Hamarneh
MICCAI 2018
https://link.springer.com/chapter/10.1007/978-3-030-00937-3_84



Izadi, Mirikhariji, Kawahara, Hamarneh
ISBI 2018
<https://ieeexplore.ieee.org/abstract/document/8363712>

hair removal



Mirzaalian, Hamarneh, Lee
IEEE TIP 2014

<https://ieeexplore.ieee.org/document/6918479/>

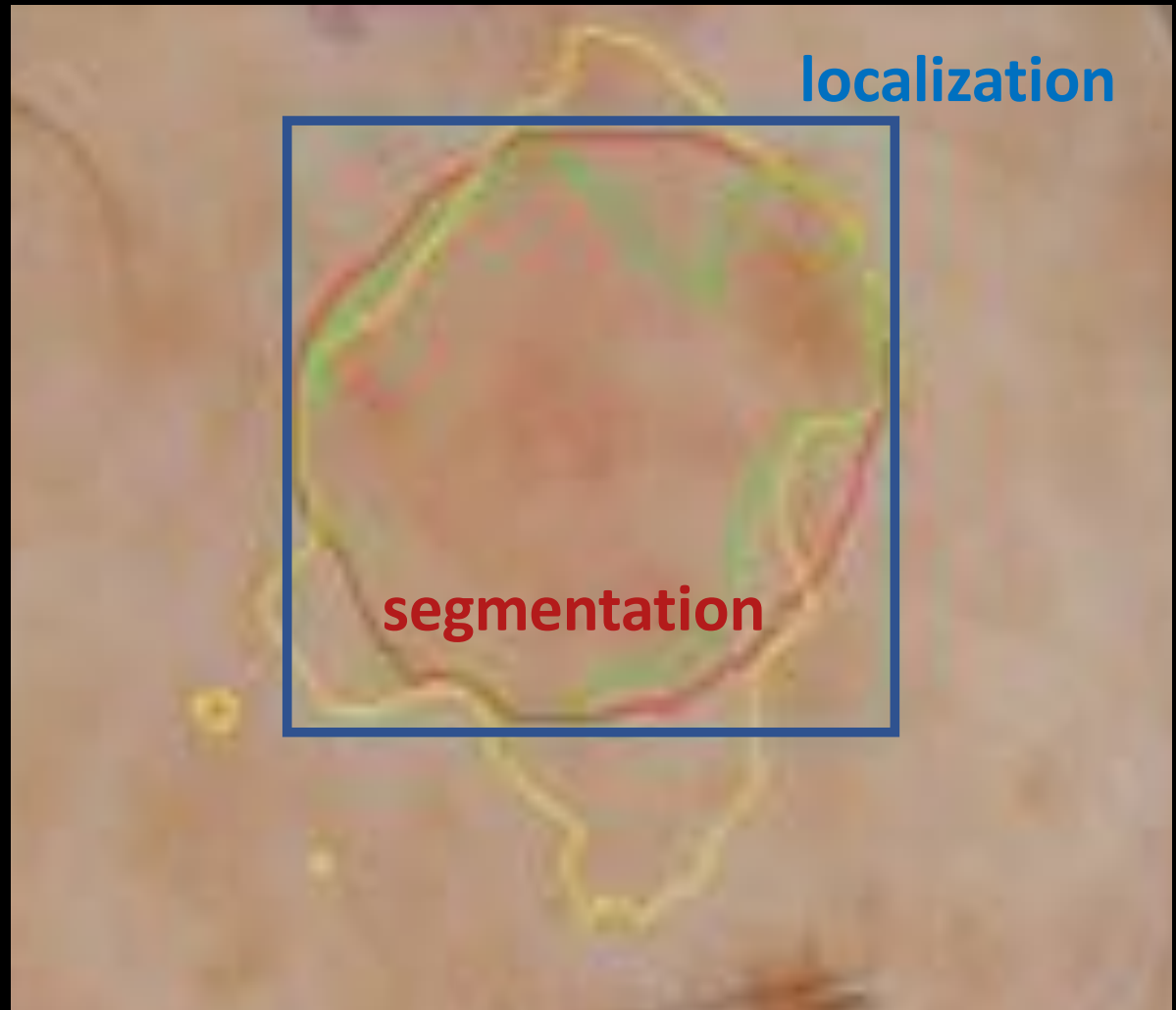
Taskonomy CVPR 2018
Zamir, Savarese, Malik

Other prediction tasks

Joint skin lesion localization
and segmentation

Vesal, Patil, Ravikuma, Maier
ISIC 2018
https://link.springer.com/chapter/10.1007/978-3-030-01201-4_31

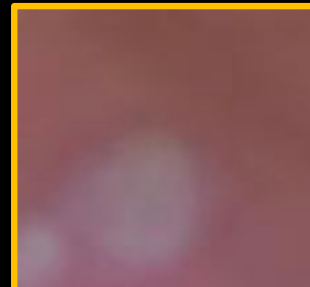
Blue: detected bounding box
Green: GT lesion boundary
Yellow: SkinNet
Red: Faster-RCNN+SkinNet



Real-life skin images



viewpoint



blur



background



over/under-exposure



Annotations



Fully- weakly- un-supervised

100 images with clean labels

vs

1000 images with noisy labels?

Adaptively handle noisy annotations
via modified deep model optimization

1. learn weight map W to control pixel contribution to loss
2. $\uparrow W \Leftrightarrow \uparrow$ agreement with clean data
agreement in loss gradient

Mirikhrajji, Yan, Hamarneh, 2019
<https://arxiv.org/abs/1906.03815>

data
100 clean
1500 noisy



original

pretrain on noisy
fine-tune on clean

78.6

Dice %

modified

N/A

80.7

76.1

80.3

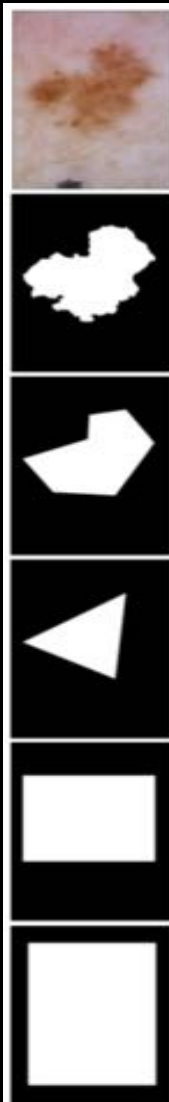
75.0

79.5

73.0

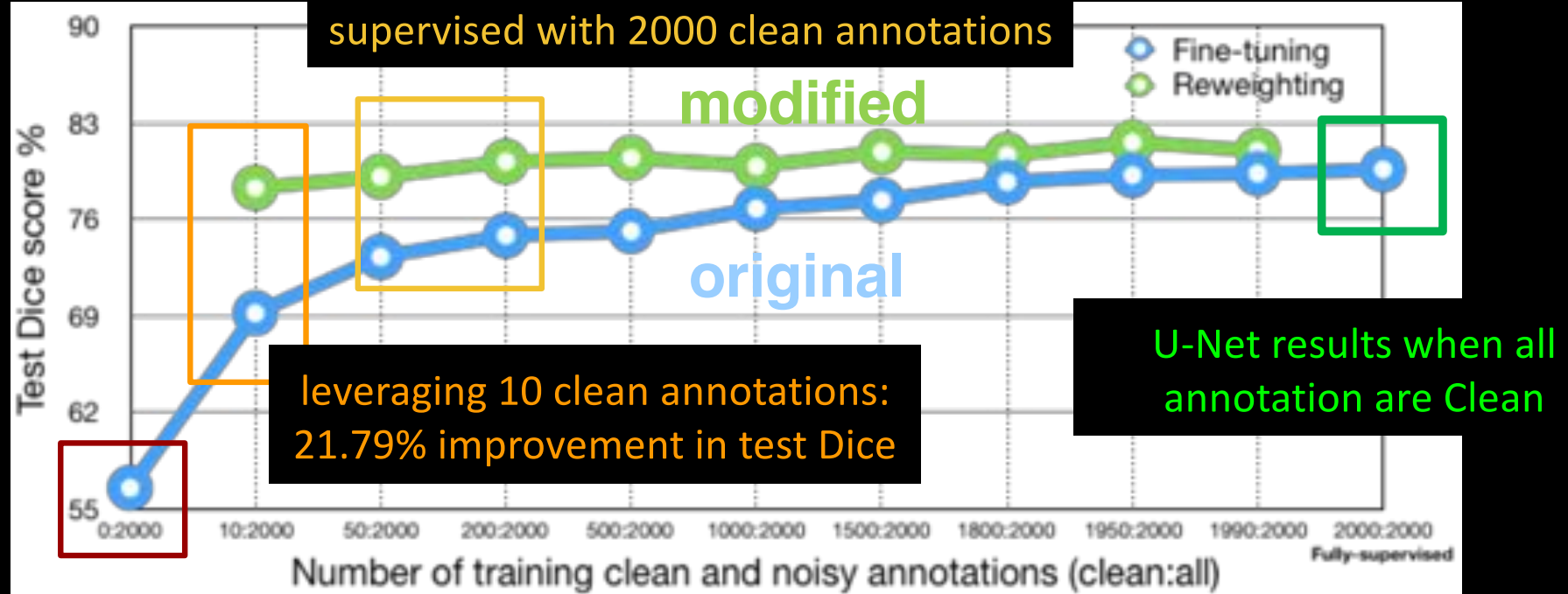
73.6

70.5



Annotations

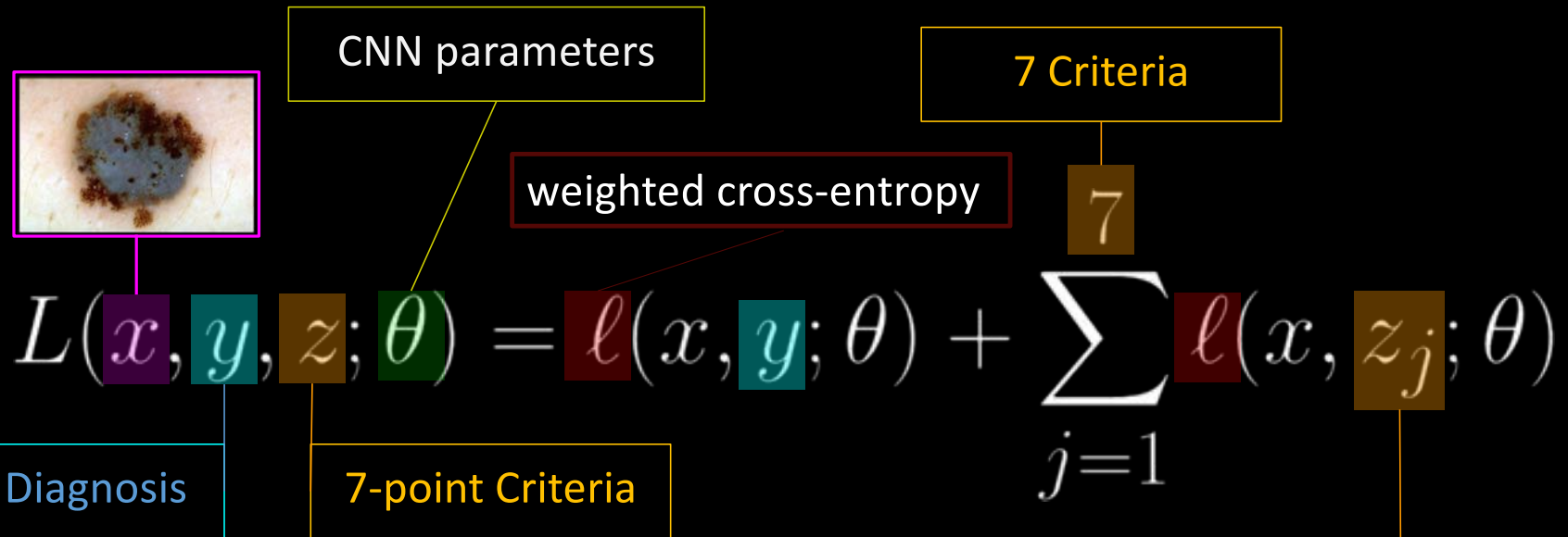
with only ~100 clean annotations, the reweighting outperforms the fully-supervised with 2000 clean annotations



U-Net results when all annotation are noisy

Loss choice

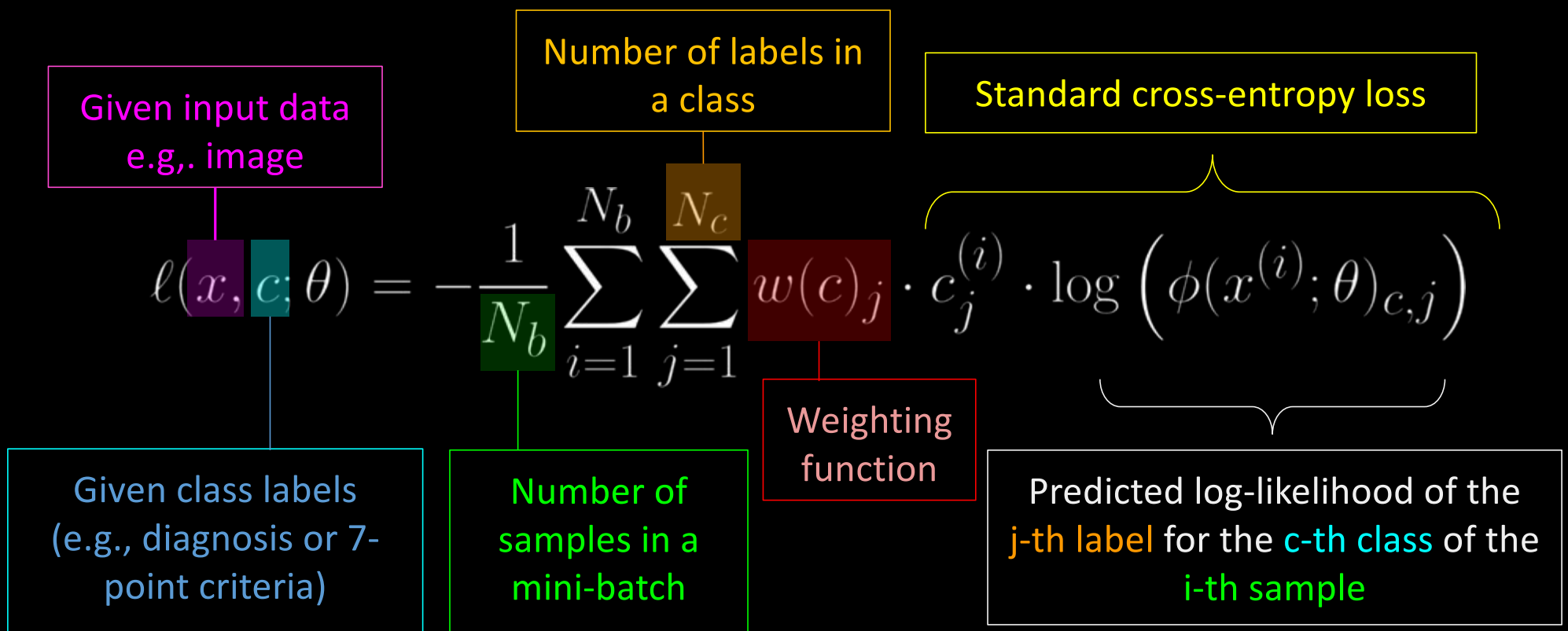
Kawahara, Daneshvar, Argenziano, Hamarneh
IEEE JBHI 2019
<https://ieeexplore.ieee.org/document/8333693>



1. Basal cell carcinoma (BCC)
2. Nevus (multiple) (NEV)
3. Melanoma (multiple) (MEL)
4. Seborrheic keratosis (SK)
5. Miscellaneous (MISC)

1. Pigment Network (PN)
2. Blue Whitish Veil (BWV)
3. Vascular Structures (VS)
4. Pigmentation (PIG)
5. Streaks (STR)
6. Dots and Globules (DaG)
7. Regression Structures (RS)

Weighted cross-entropy loss

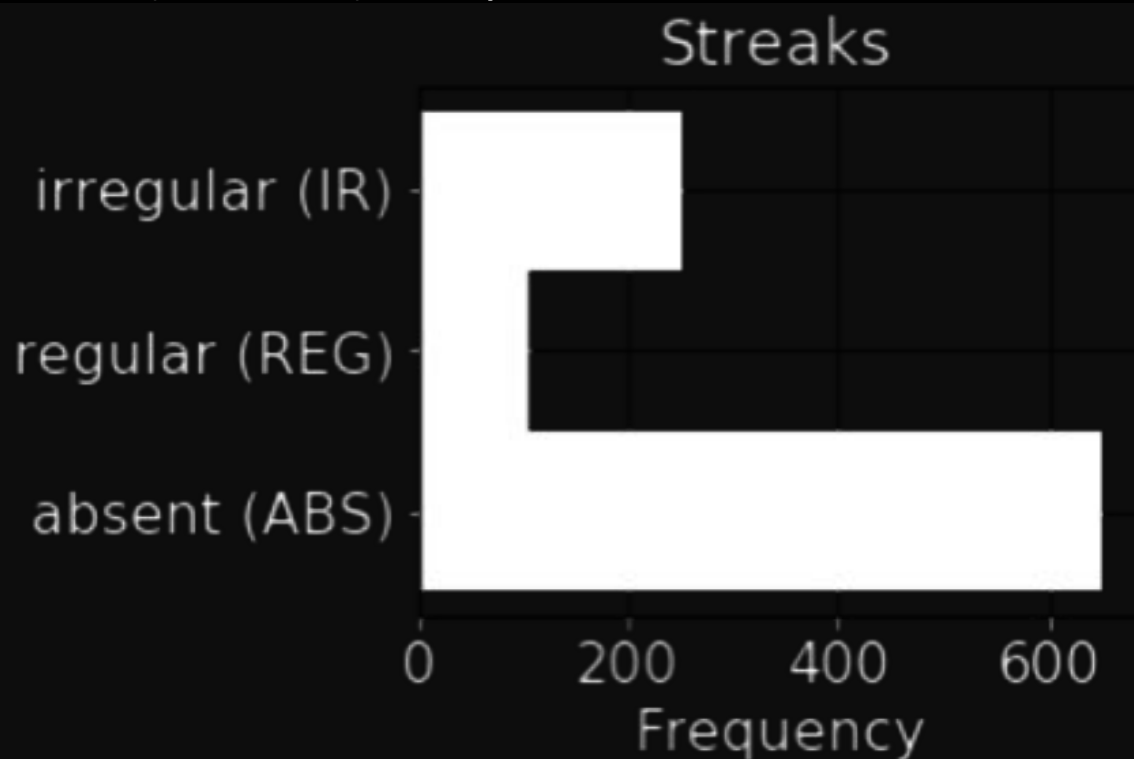


Class imbalance

Context: Melanoma diagnosis; 7 dermoscopic criteria

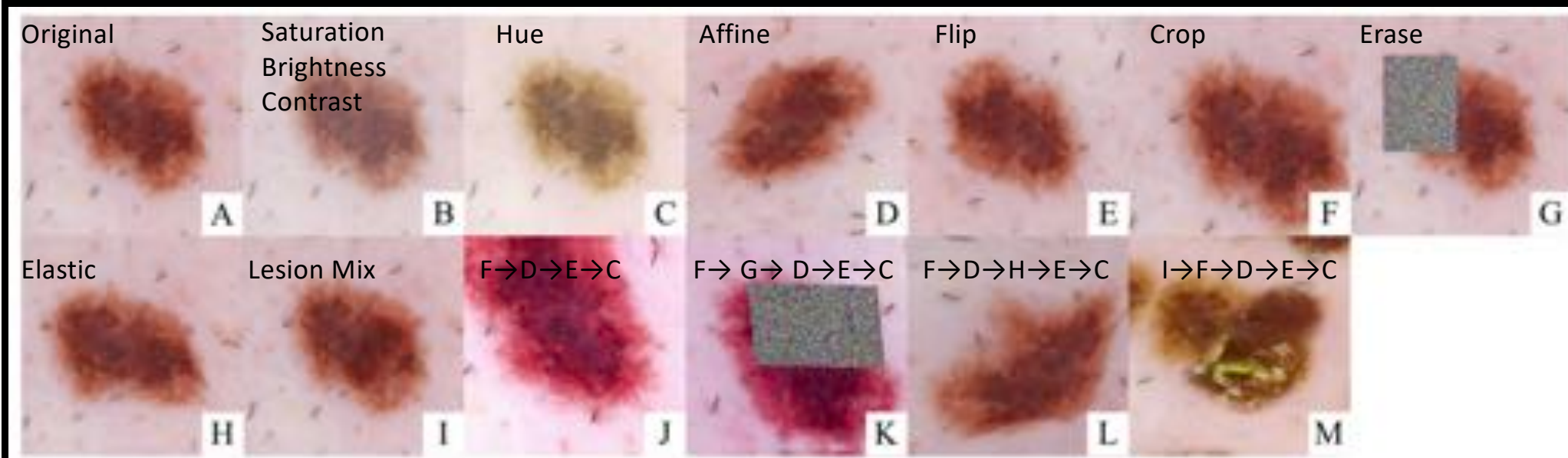
Ensure each mini-batch includes $\geq k$ (random) samples from each label

1. Pigment Network (PN)
2. Blue Whitish Veil (BWV)
3. Vascular Structures (VS)
4. Pigmentation (PIG)
5. Streaks (STR)
6. Dots and Globules (DaG)
7. Regression Structures (RS)



Higher cross entropy weights assigned to infrequent labels in a mini-batch

Data augmentation



Data Augmentation for Skin Lesion Analysis

Perez, Vasconcelos, Avila, Valle

ISIC 2018

https://link.springer.com/chapter/10.1007/978-3-030-01201-4_33

Data augmentation

Simulation via Physically- and Statistically-based Warps

DeformIt

MICCAI 2008

Hamarneh, Jassi, Tang, Booth

https://link.springer.com/chapter/10.1007/978-3-540-85988-8_55

<https://ieeexplore.ieee.org/document/6867974>

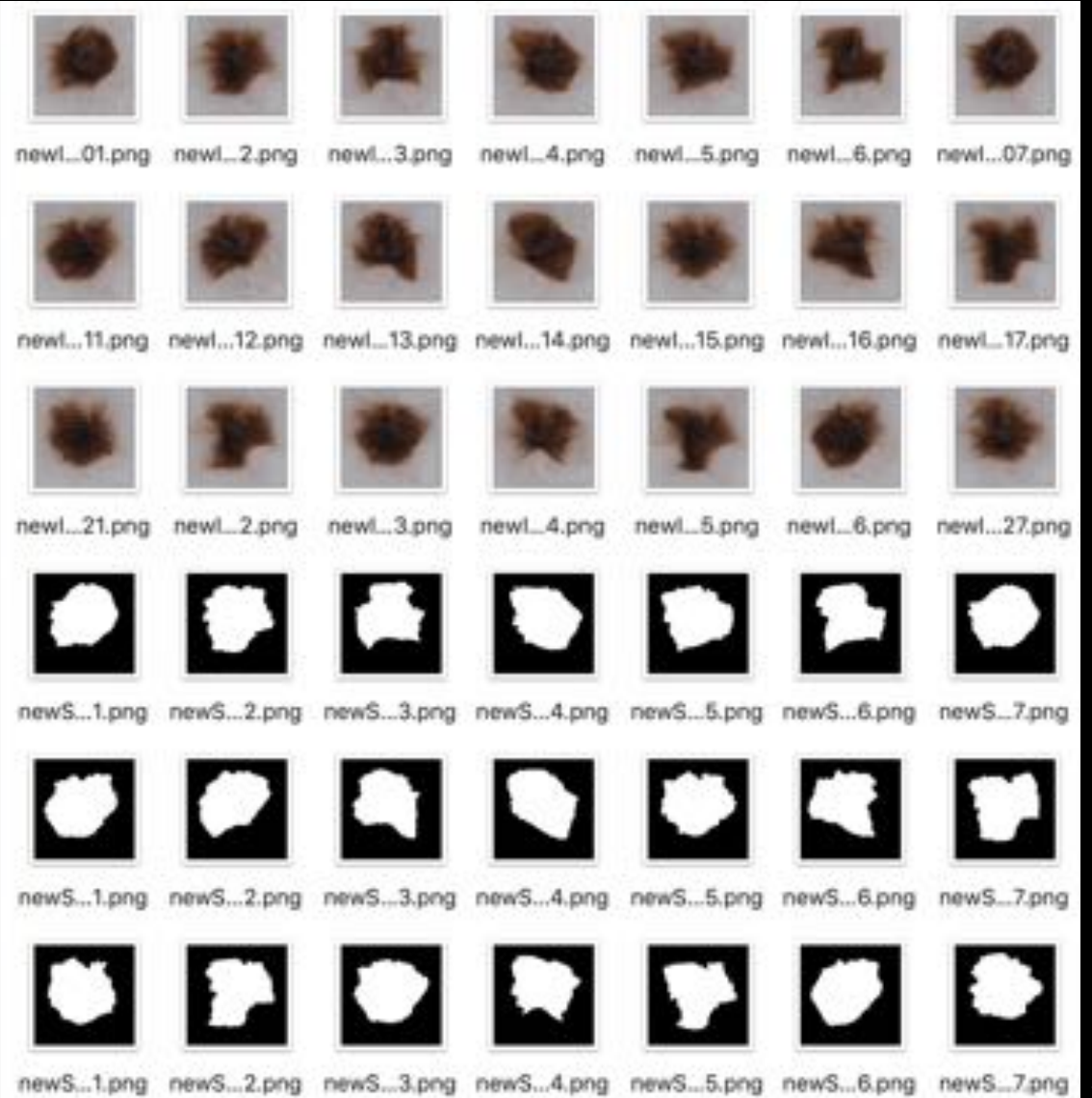
$$I = \bar{I} + \alpha \mathbf{Pb} + (1 - \alpha) \Phi \mathbf{u}$$

variational
PCA

Vibrational
FEM

\uparrow data \rightarrow $\uparrow\alpha$

rely more on statistical model and less on knowledge-based models



Augmentation

Hair Occlusion Simulator

HairSim

IEEE TIP 2014

Mirzaalian, Lee , Hamarneh

<https://ieeexplore.ieee.org/document/6918479>

- medial A-B curve synthesizer
- hair-thickening: dilation radius \propto geodesic distance to A and B

$$r(p) = \min\{T, \alpha\Gamma(p, A), \alpha\Gamma(p, B)\}$$

- New image (H): blending of clean image I with a colored C hair mask M , Hair color C

$$\begin{bmatrix} H_R \\ H_G \\ H_B \end{bmatrix} = I(\mathbf{1} - G_\sigma * M) + \begin{bmatrix} C_R \\ C_G \\ C_B \end{bmatrix} (G_\sigma * M)$$



Augmentation

Generative Adversarial Networks GANS

Generating Highly Realistic Images of Skin Lesions with GANs (MelanoGan)

Baur, Albarqouni, Navab ISIC 2018

https://link.springer.com/chapter/10.1007/978-3-030-01201-4_28

<https://arxiv.org/abs/1804.04338>

Skin Lesion Synthesis with GANs

Bissoto, Perez, Valle, Avila, ISIC 2018

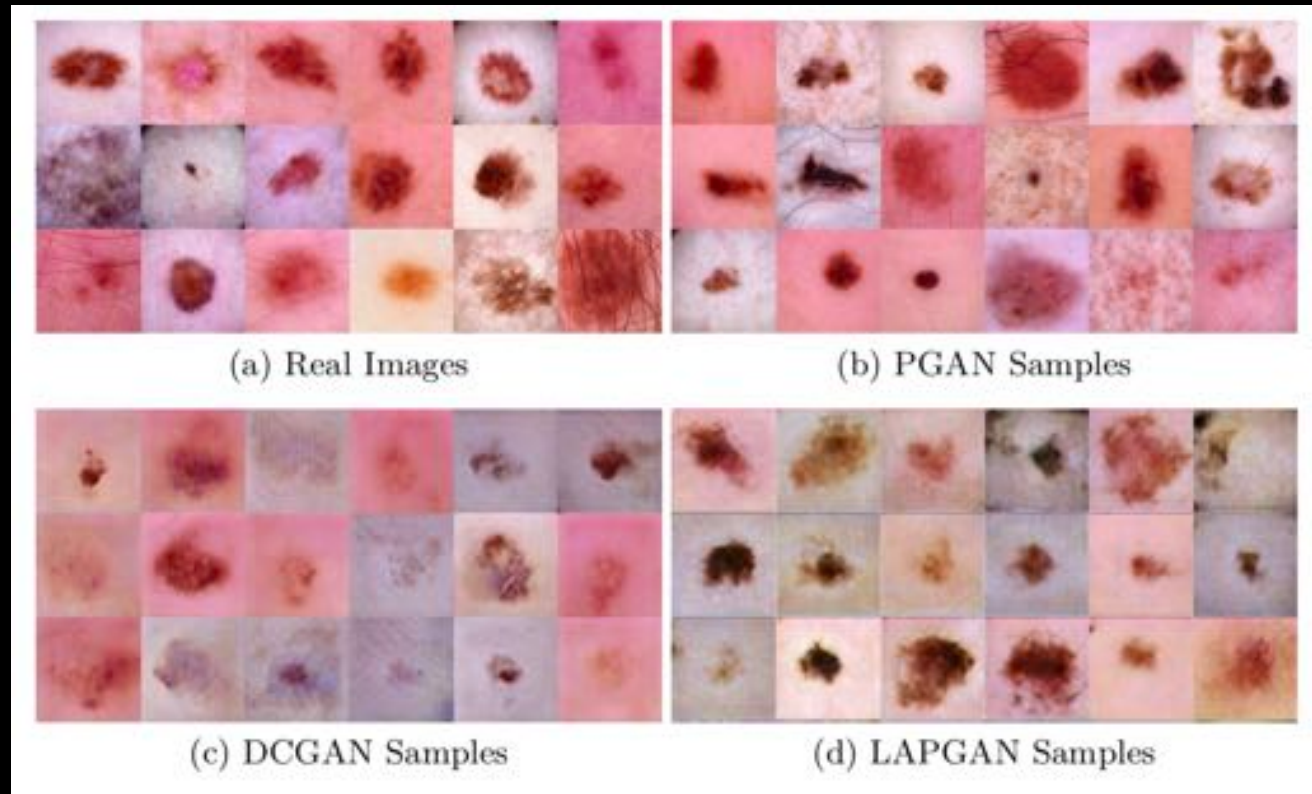
https://link.springer.com/chapter/10.1007/978-3-030-01201-4_32

Augmenting data with GANs to segment melanoma skin lesions

Pollastri, Bolelli, Paredes, Grana

Multimedia Tools and Applications 2019

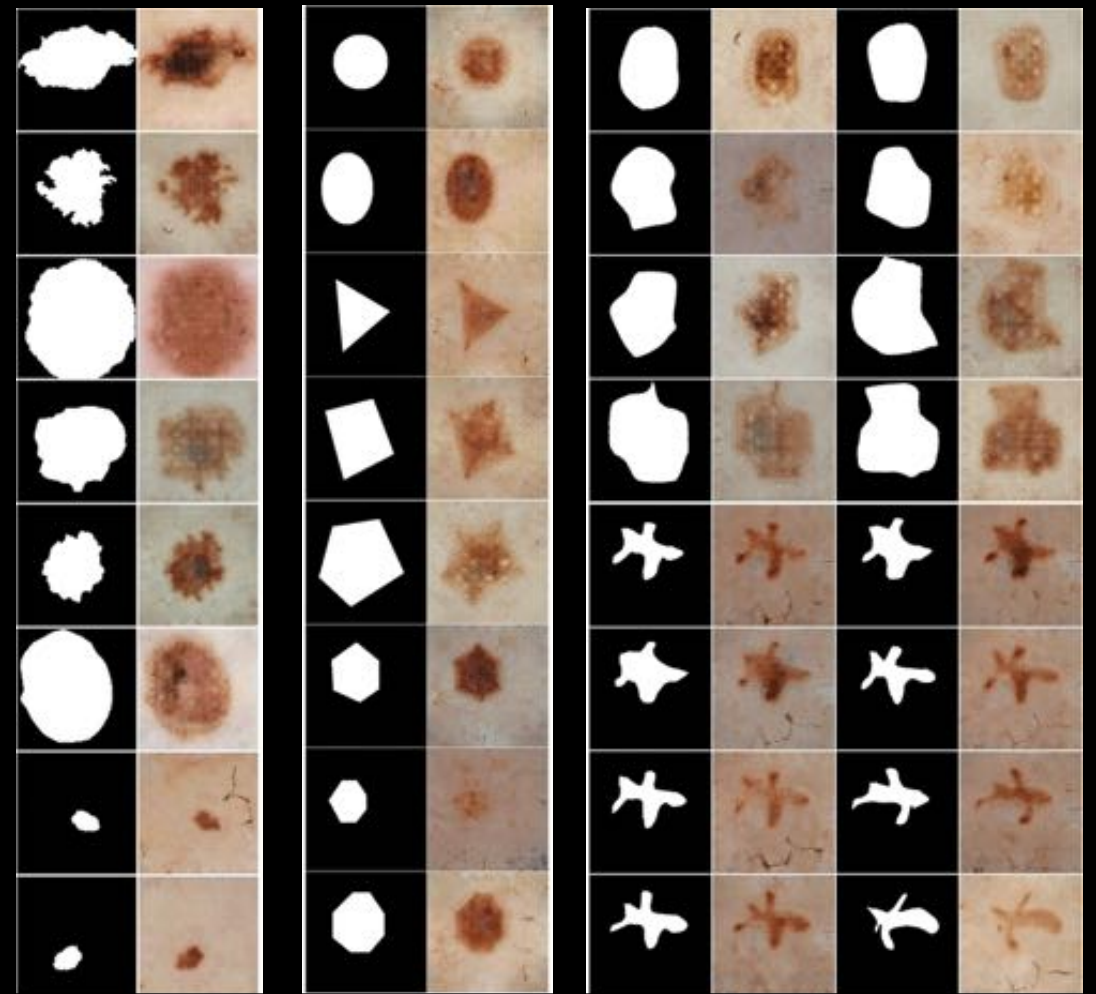
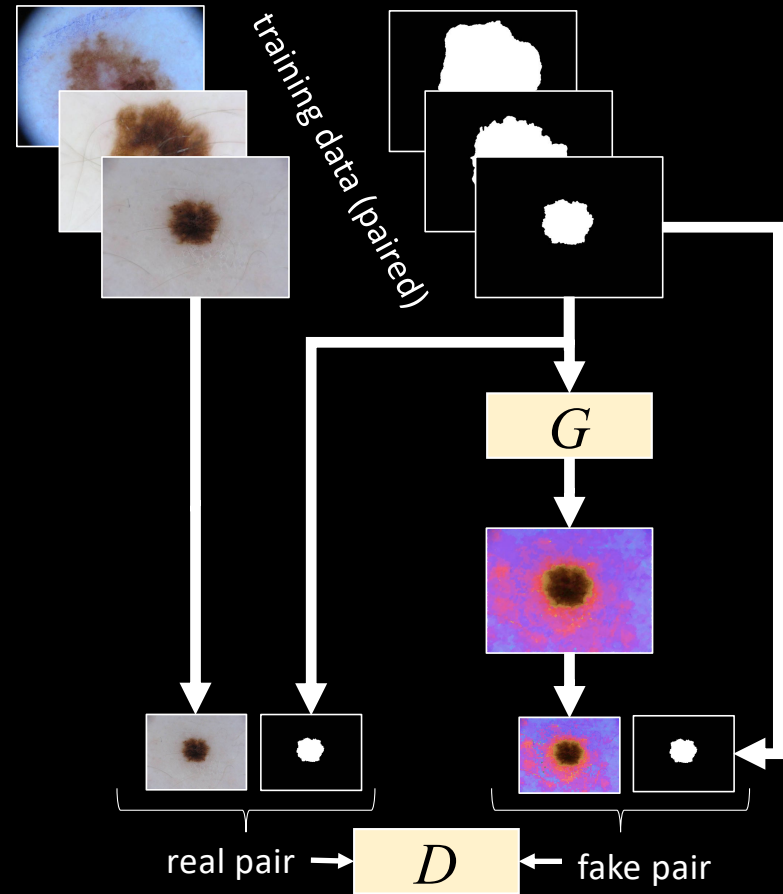
<https://link.springer.com/article/10.1007/s11042-019-7717-y>



Augmentation

GAN-based **Mask2Lesion** translation
Abhishek, Hamarneh. 2019

<https://arxiv.org/abs/1906.05845>

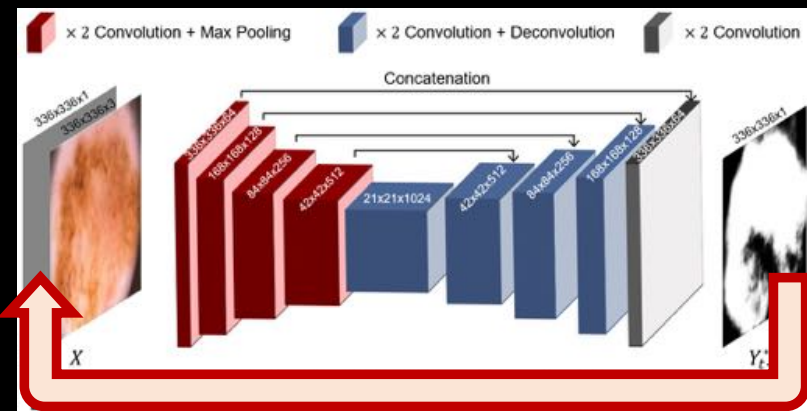


Network architecture

Deep **auto-context** FCN for skin lesion segmentation

Mirikhrajji, Izadi, Kawahara, Hamarneh ISBI2018

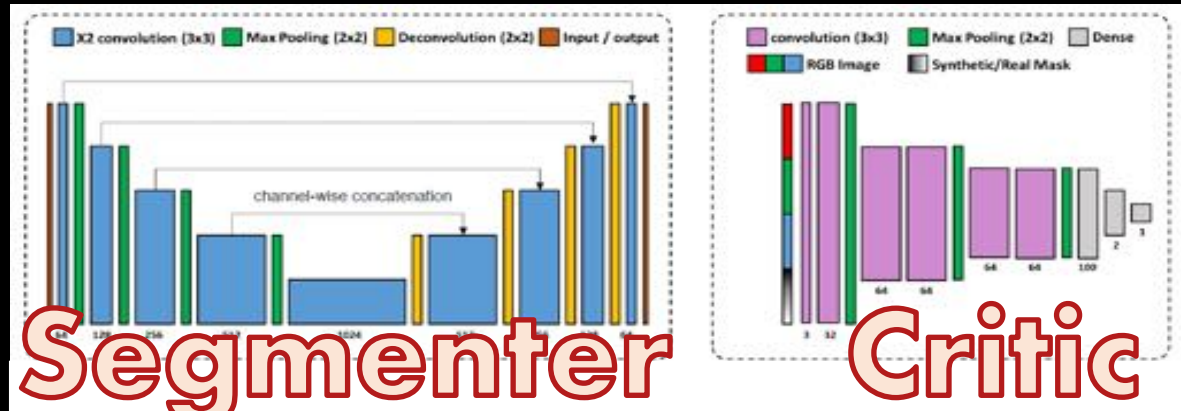
<https://ieeexplore.ieee.org/document/8363711>



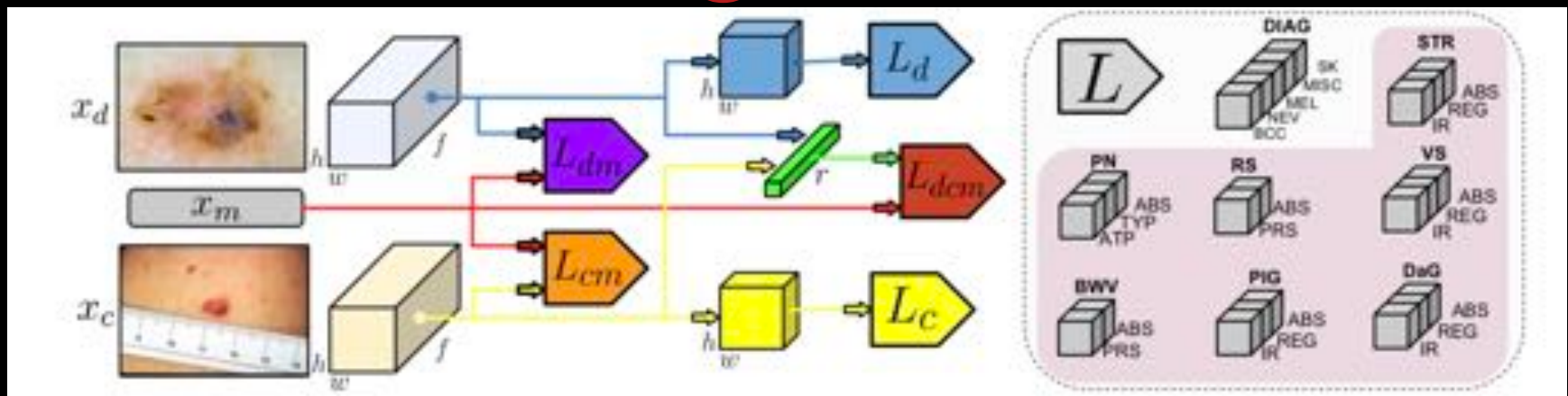
Generative **adversarial** networks to segment skin lesions

Izadi, Mirikhrajji, Kawahara, Hamarneh ISBI 2018

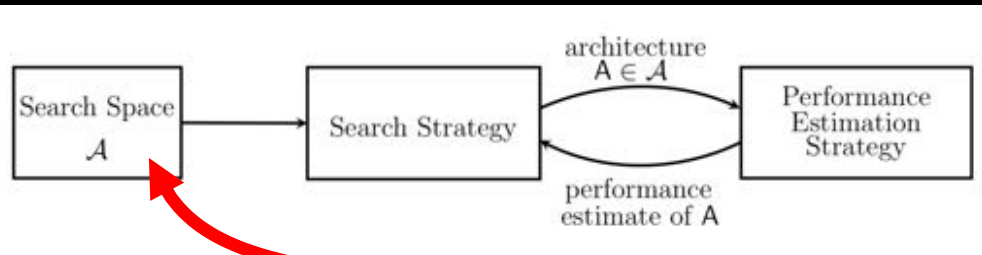
<https://ieeexplore.ieee.org/abstract/document/8363712>



diagnosis &
7-point derm.
criteria



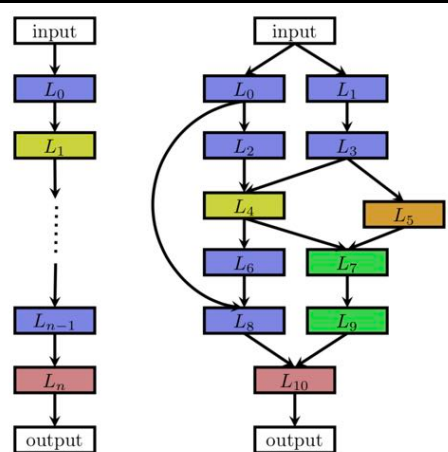
Network architecture search (NAS)



Neural Architecture Search: A Survey

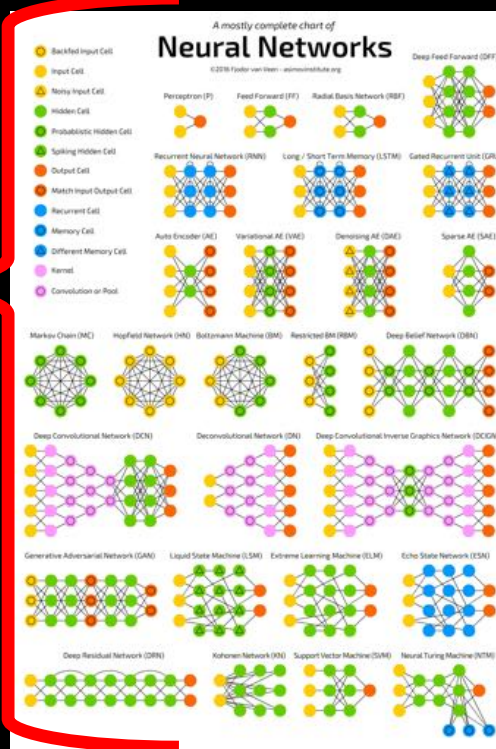
Thomas Elsken, Jan Hendrik Metzen, Frank Hutter; 20(55):1–21, 2019

<https://arxiv.org/abs/1808.05377>

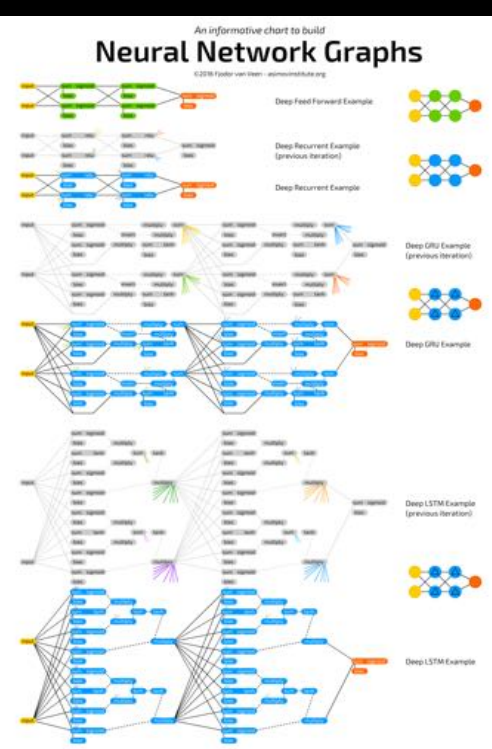


Arrangement of layers

or blocks of layers



© Fjodor Van Veen, The Asimov Institute, 2017
<https://www.asimovinstitute.org/author/fjodorvanveen>

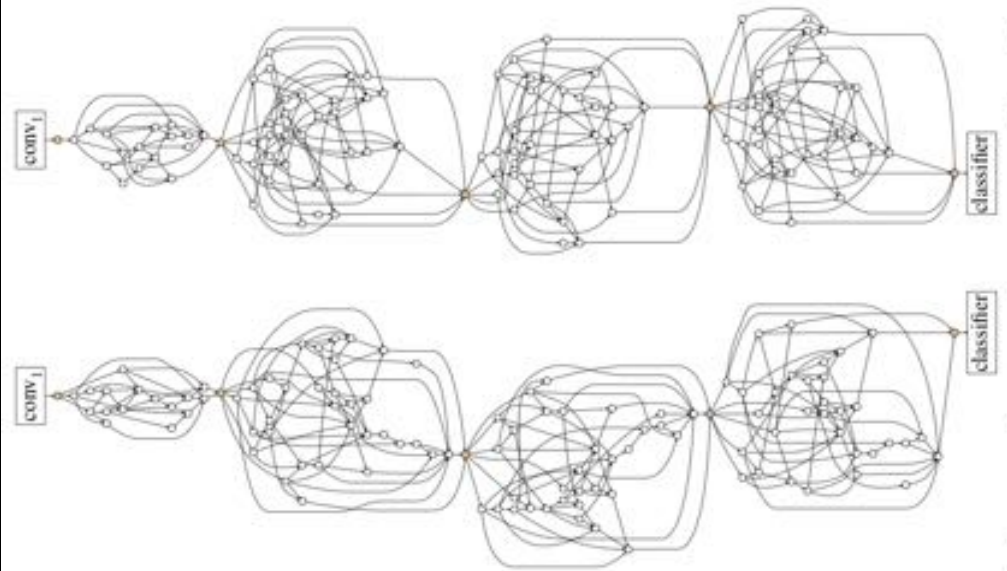


Network architecture search (NAS)

Exploring Randomly Wired Neural Networks for Image Recognition

Saining Xie Alexander Kirillov Ross Girshick Kaiming He

Facebook AI Research (FAIR)



Exploring Randomly Wired Neural Networks for Image Recognition

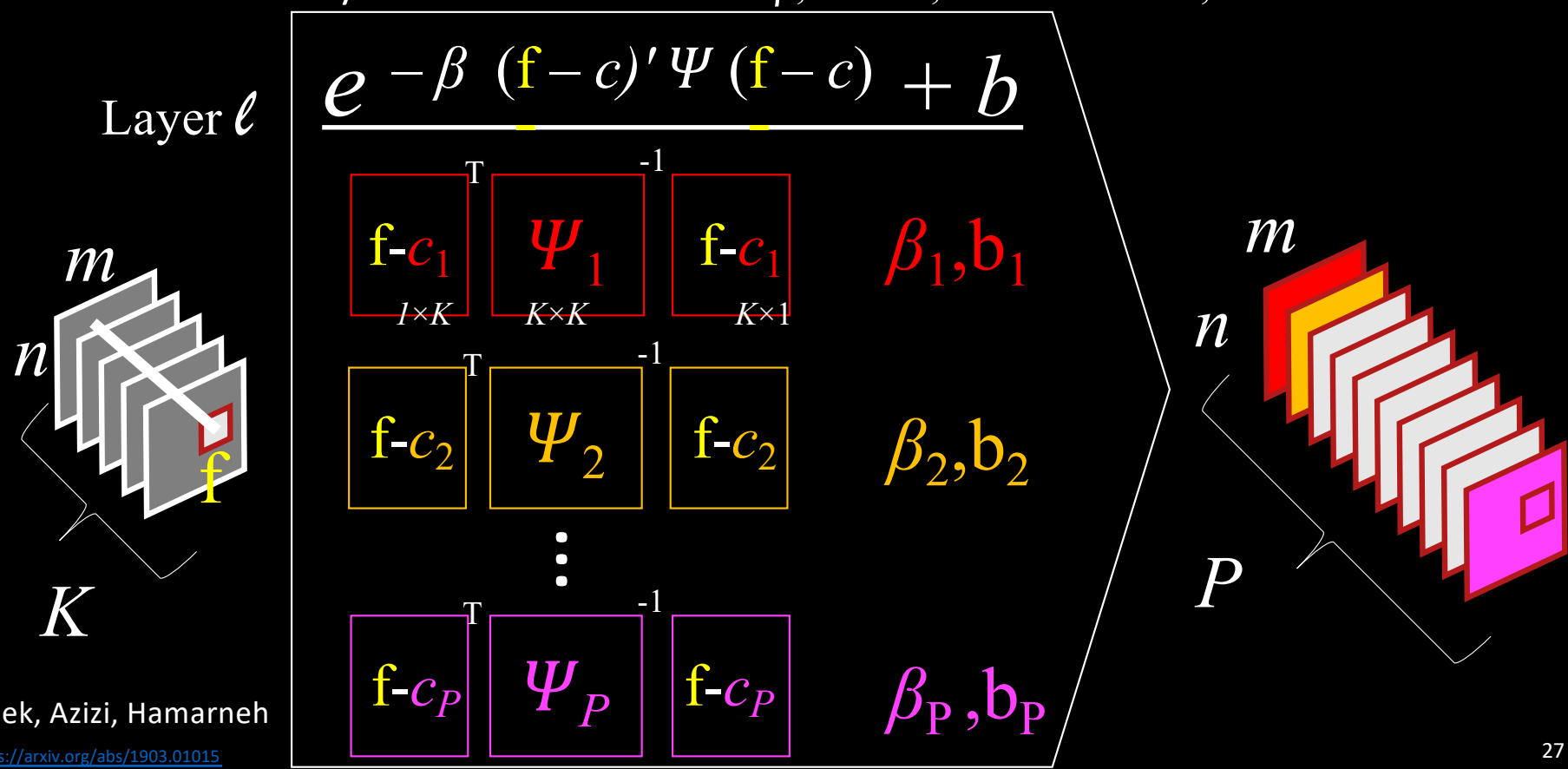
Xie, Kirillov, Girshick, He 2019

<https://arxiv.org/abs/1904.01569>

Layer design

Layers: [de]conv, fully conn., [un]pool, sequence eg LSTM, activation eg RELU

Radial Basis Function RBF layer with learnable width β , center c , transformation Ψ , bias b



Layer design

Radial Basis Function RBF layer with learnable width β , center c , transformation Ψ , bias b

0	1	2	3	4	5	6	7	8	9
0	1	2	3	4	5	6	7	8	9
0	1	2	3	4	5	6	7	8	9
0	1	2	3	4	5	6	7	8	9
0	1	2	3	4	5	6	7	8	9
0	1	2	3	4	5	6	7	8	9
0	1	2	3	4	5	6	7	8	9
0	1	2	3	4	5	6	7	8	9
0	1	2	3	4	5	6	7	8	9
0	1	2	3	4	5	6	7	8	9

t-SNE 3rd layer

Without RBF



with RBF

Adversarial attacks

Original image



Benign
Malignant

Adversarial noise



+ 0.04 ×

Imperceptible changes to images crafted to
make DNNs produce specific output

Adversarial example



Benign
Malignant

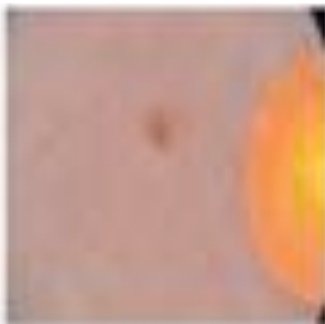
Finlayson, Bowers, Ito, Zittrain,
Beam, Kohane
Science 2019

<https://science.scienmag.org/content/363/6433/1287>

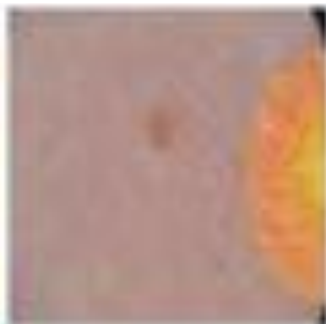
Asgari, Abhishek, Azizi,
Hamarneh
CVPR 2019

<https://arxiv.org/abs/1903.01015>

Legitimate



Perturbed



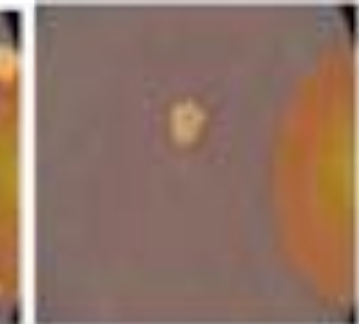
GT Seg



UNet Seg.



Ours/RBF



Dataset shift

Bias and fairness

Machine Learning and Health Care Disparities in Dermatology

Unfortunately, most ML programs are largely learning on light skin. For example, in the International Skin Imaging Collaboration: Melanoma Project, which is one of the largest and often-used, open-source, public-access archives of pigmented lesions, much of the patient data are heavily collected from fair-skinned populations in the United States, Europe, and Australia.³ Thus, no matter how advanced the ML algorithm, it may underperform on images of lesions in skin of color.

JAMA Dermatology 2018;154(11)

Adamson, Smith

<https://jamanetwork.com/journals/jamadermatology/article-abstract/2688587>

ORIGINAL ARTICLE



Classification of the Clinical Images for Benign and Malignant Cutaneous Tumors Using a Deep Learning Algorithm

Seung Seog Han^{1,7}, Myoung Shin Kim^{2,7}, Woohyung Lim³, Gyeong Hun Park⁴, Ilwoo Park⁵ and Sung Eun Chang⁶

Because of the different patient demographics in the three validation datasets we tested with our algorithm, the sensitivity and specificity of these datasets were analyzed over a change in threshold from 0.0000 to 1.0000 (Figure 4). The sensitivities of the Asan and Hallym test dataset over this threshold were similar. However, the specificities for BCC, squamous cell carcinoma, and melanoma between the Asan test dataset and Edinburgh dataset showed substantial differences, which may have been due to malignancy subtypes and the skin colors around the lesions. It may be necessary, therefore, to choose different thresholds or generate different models for different ethnic groups.

Journal of Investigative Dermatology 2018; 138(7)

Han et al.

<https://jamanetwork.com/journals/jamadermatology/article-abstract/2688587>

Dataset shift

Bias and fairness

Test dataset of European population:
10 classes - 1300 images

Train and test on same dataset

Deep features to classify skin lesions

Kawahara, BenTaieb, Hamarneh

ISBI 2016

<https://ieeexplore.ieee.org/document/7493528>

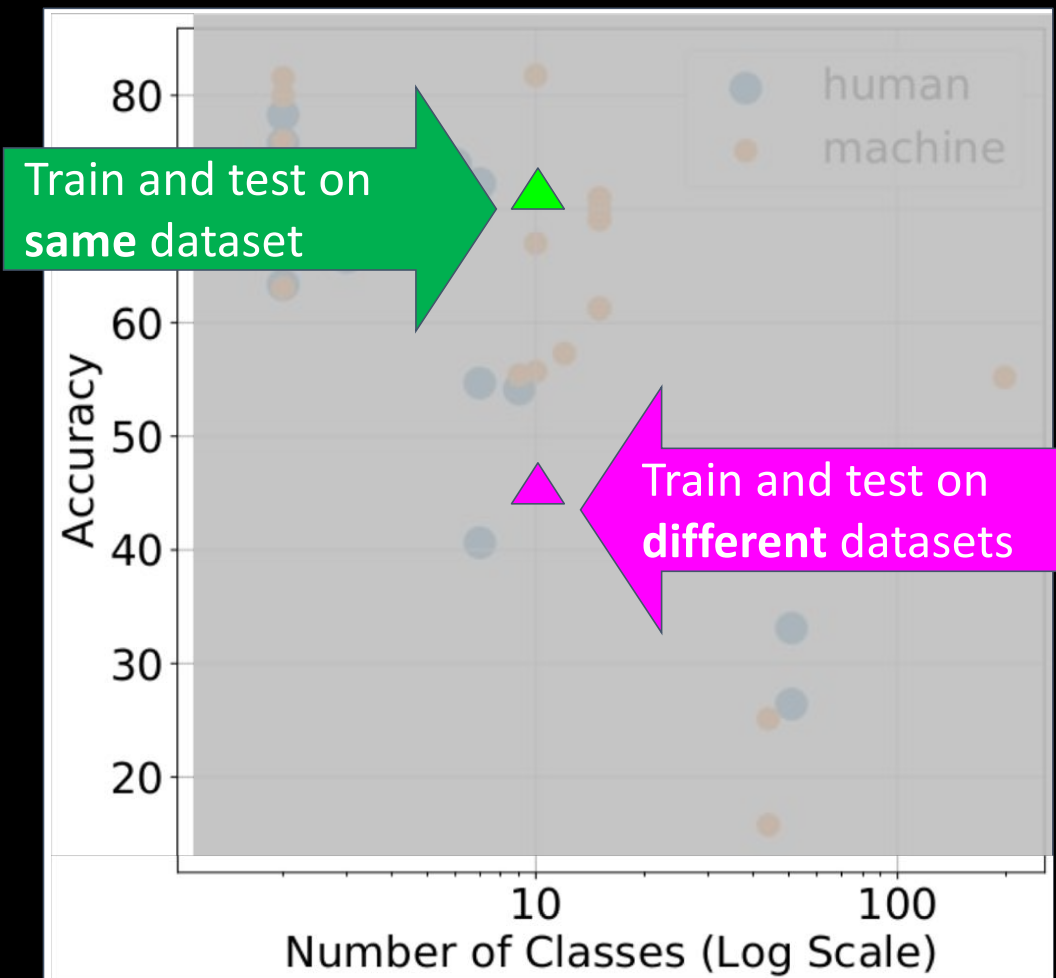
Train on Asian, test on European

Classification of the Clinical Images for Benign and Malignant Cutaneous Tumors Using a Deep Learning Algorithms

Han, Kim, Lim, Park, Park, Chang

Journal of Investigative Dermatology

[https://www.jidonline.org/article/S0022-202X\(18\)30111-8/](https://www.jidonline.org/article/S0022-202X(18)30111-8/)



Dataset shift

MICCAI 2019 Yoon, Hamarneh, Garbi

7 Domains:

1 primary: HAM10000

6 secondary: Dermofit+MSK+UDA+
ONIC+Derm7pt+PH2
 n_s samples/class

CCSA loss: classification &
contrastive semantic alignment

[Motiian ICCV 2017] CE loss + feature
alignment/separation losses

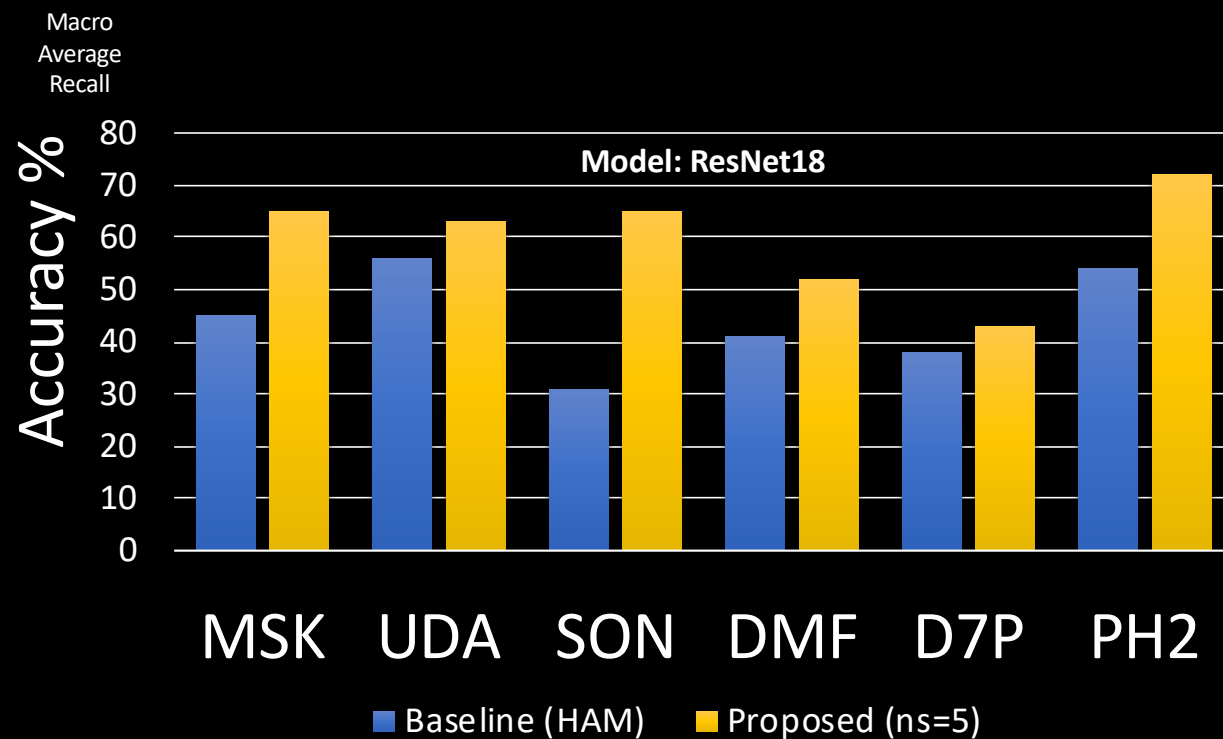
Class imbalance:

Intra-domain

$P(\text{nevus}) \gg P(\text{melanoma})$

Inter-domain

dermatofibroma \notin Domain2



Dynamic sampling

two image-label pairs across domain: $(x_1, y_1), (x_2, y_2)$

Adaptive weighting

of CCSA loss based on $P(y = c_i)$ and $P(y_1 = c_i, y_2 = c_j)$

Interpretability / explainability

Activation and attention maps



Selvaraju, Cogswell, Das, Vedantam, Parikh, Batra. Grad-CAM. ICCV 2017

Melanoma Recognition via Visual Attention

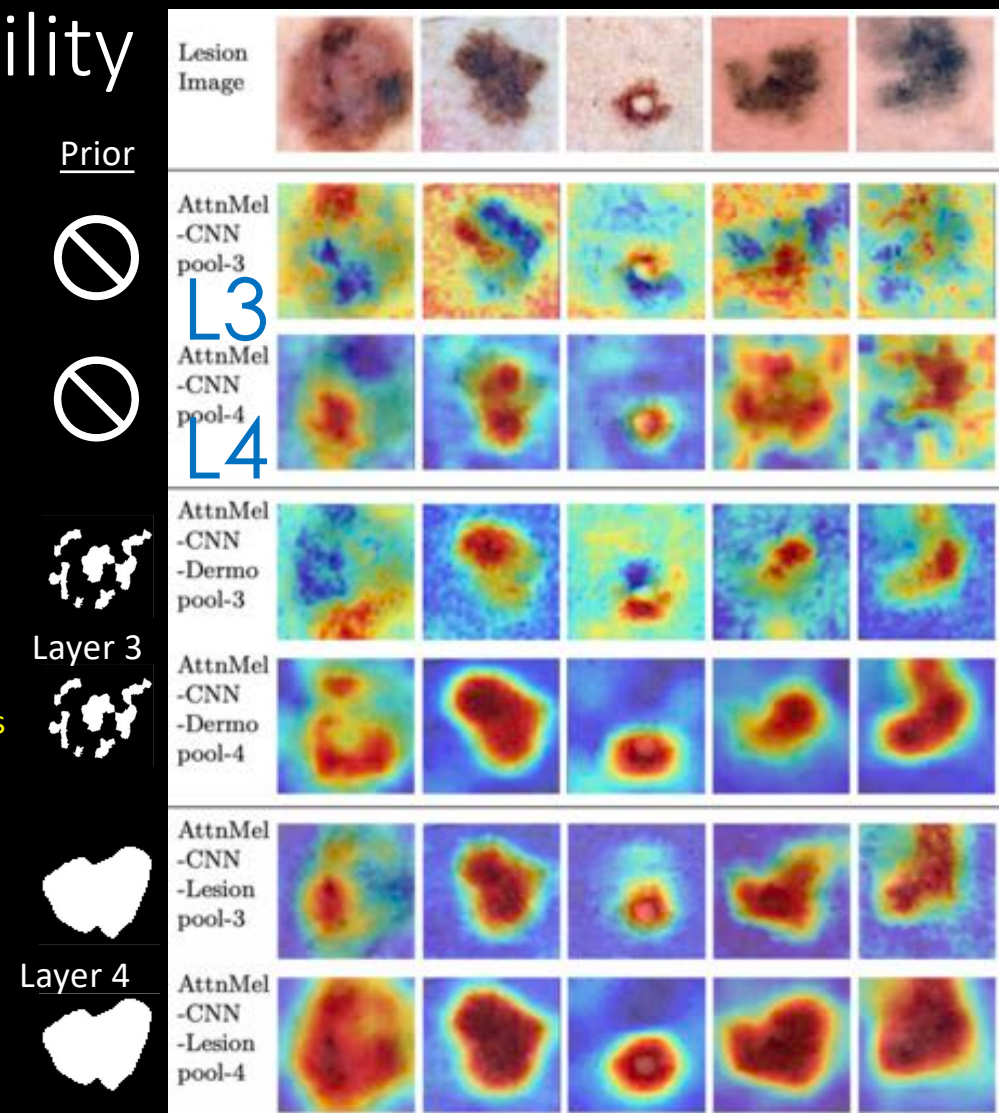
Yan, Kawahara, Hamarneh. IPMI 2019

https://link.springer.com/chapter/10.1007/978-3-030-20351-1_62

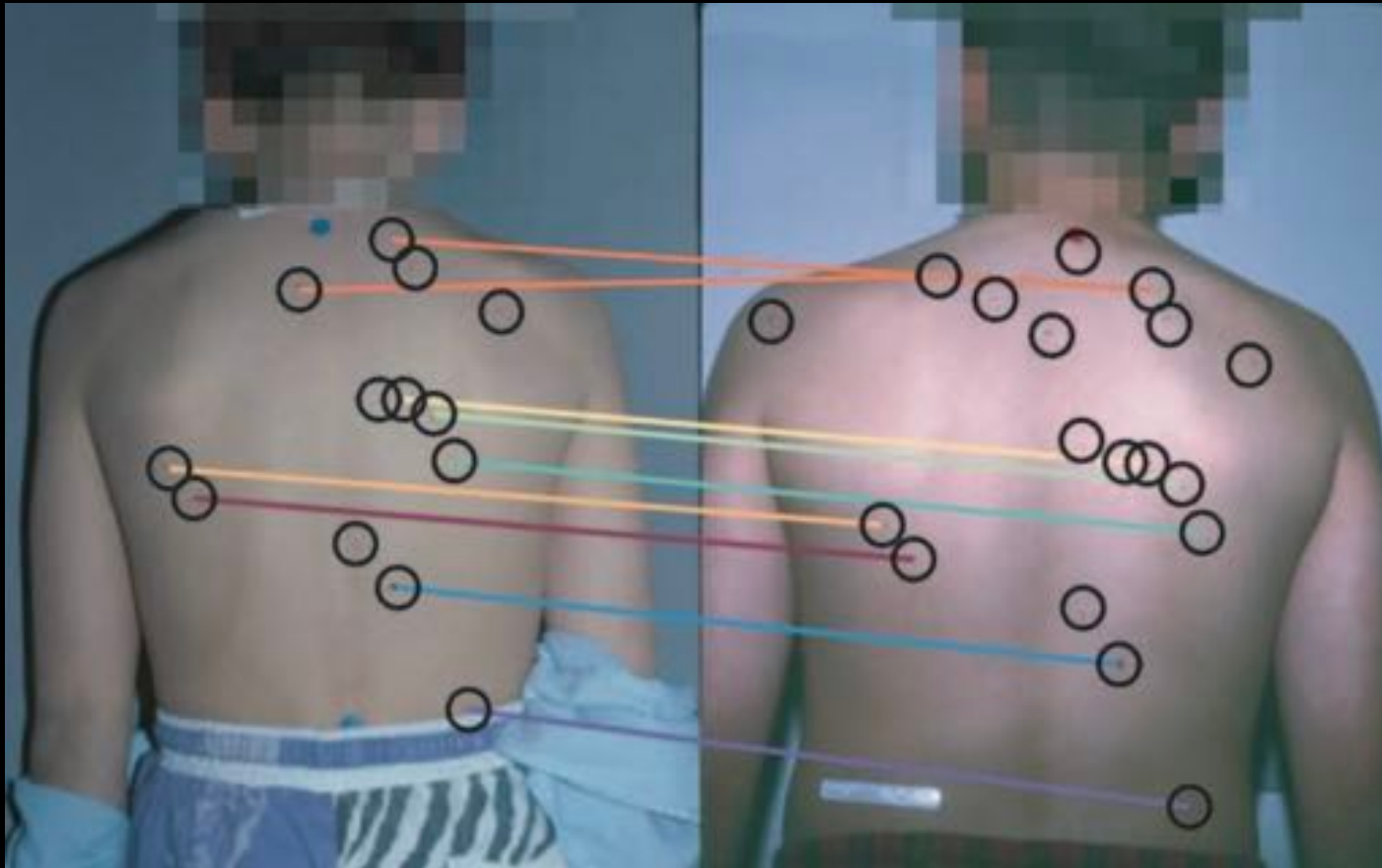
Guide (add prior to) the
attention maps to ROIs
known to discriminatory:

$$\mathcal{L}_D(\mathcal{A}, \bar{\mathcal{A}}) = 1 - D(\mathcal{A}, \bar{\mathcal{A}})$$

$$\mathcal{L} = \mathcal{L}_{focal} + \lambda_1 \mathcal{L}_D(\mathcal{A}^{(3)}, \bar{\mathcal{A}}^{(3)}) + \lambda_2 \mathcal{L}_D(\mathcal{A}^{(4)}, \bar{\mathcal{A}}^{(4)})$$



Longitudinal tracking



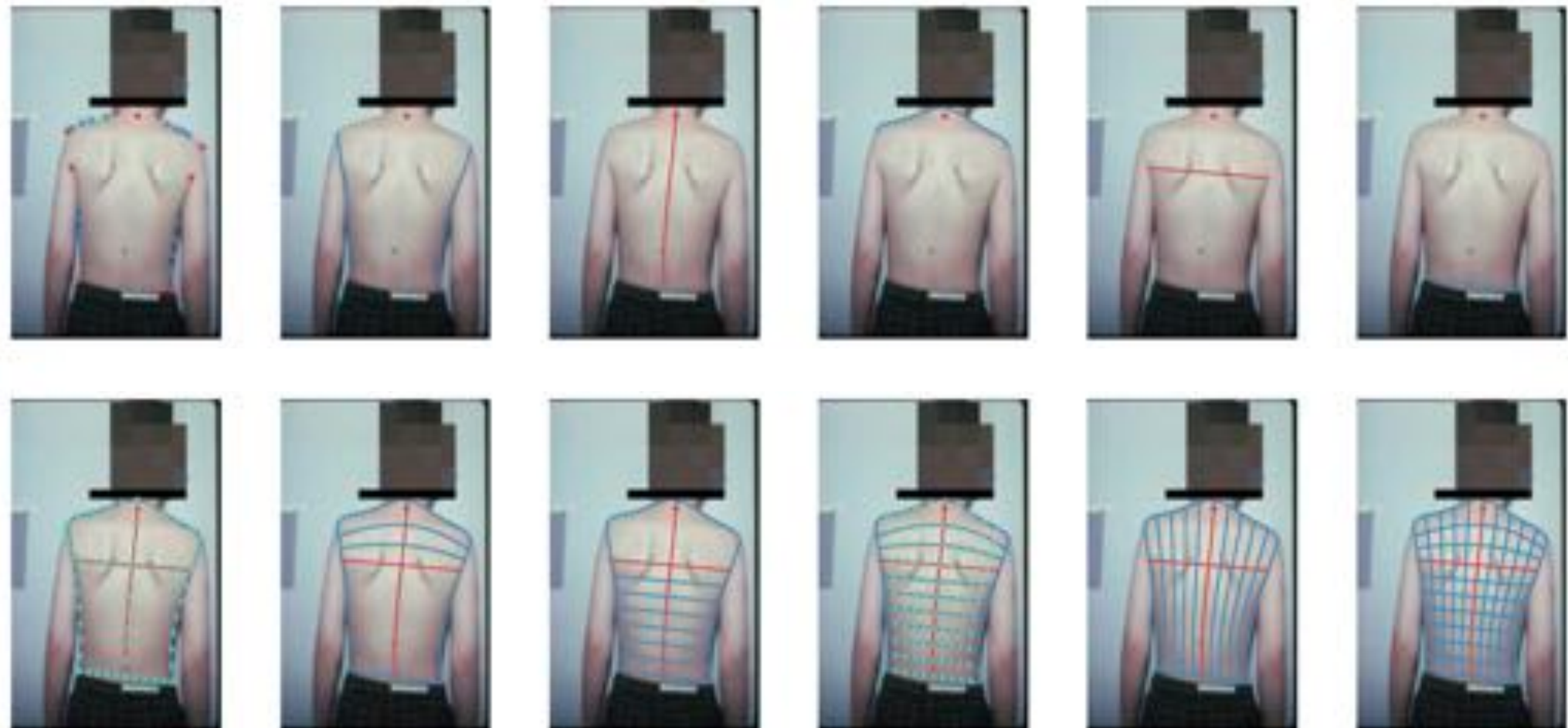
Mirzaalian, Lee, Hamarneh

CVPR 2009, MICCAI 2012, JBHI 2013, Media 2015, ISBI2015

<https://ieeexplore.ieee.org/abstract/document/5206725> <https://ieeexplore.ieee.org/document/6681908/>

<https://www.sciencedirect.com/science/article/pii/S1361841515000353> <https://ieeexplore.ieee.org/document/7164139>

Longitudinal tracking



Longitudinal tracking



Visual communication

Beyond reporting predicted class and probabilities

Image Content-Based Navigation of Skin Conditions

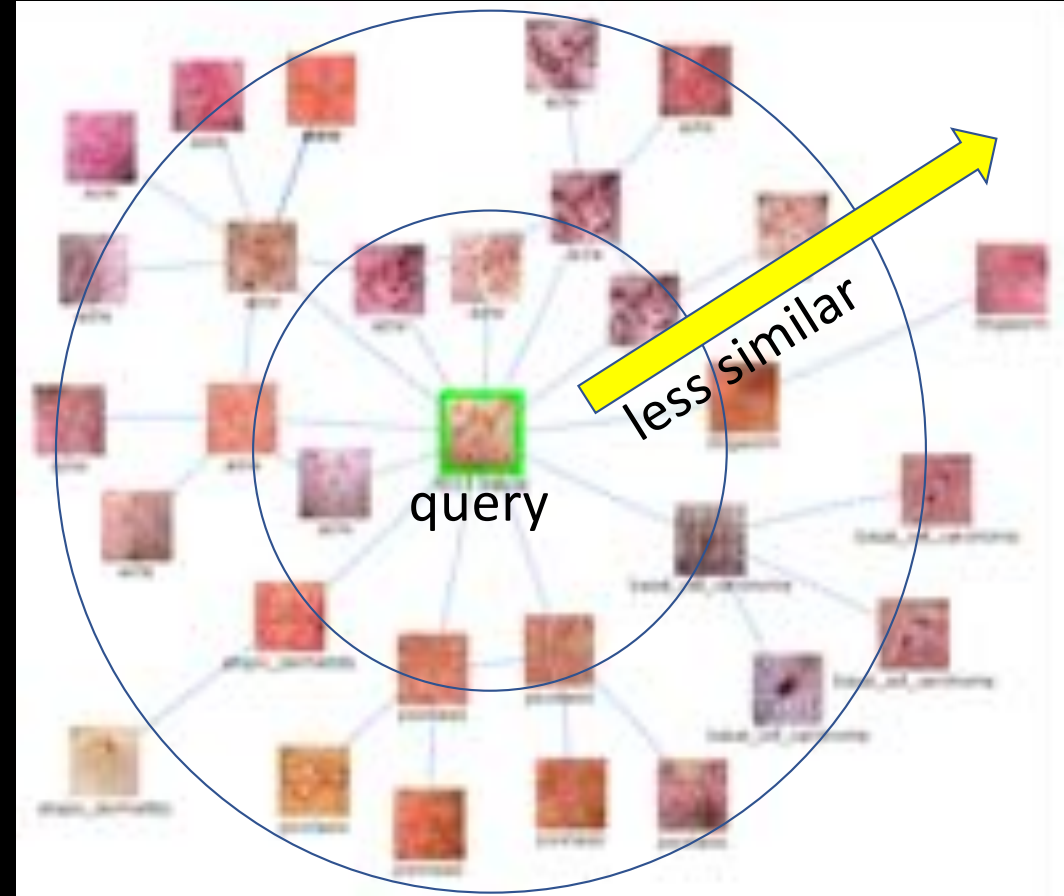
Kawahara, Hamarneh. WCD 2015

<https://www.cs.sfu.ca/~hamarneh/ecopy/wcd2015a.pdf>

Graph Geodesics to Find Progressively Similar Skin Lesion Images

Kawahara, Moriarty, Hamarneh. MICCAI GRAIL 2017

https://link.springer.com/chapter/10.1007/978-3-319-67675-3_4



CN

CN

CN

CN

MEL

MEL

MEL

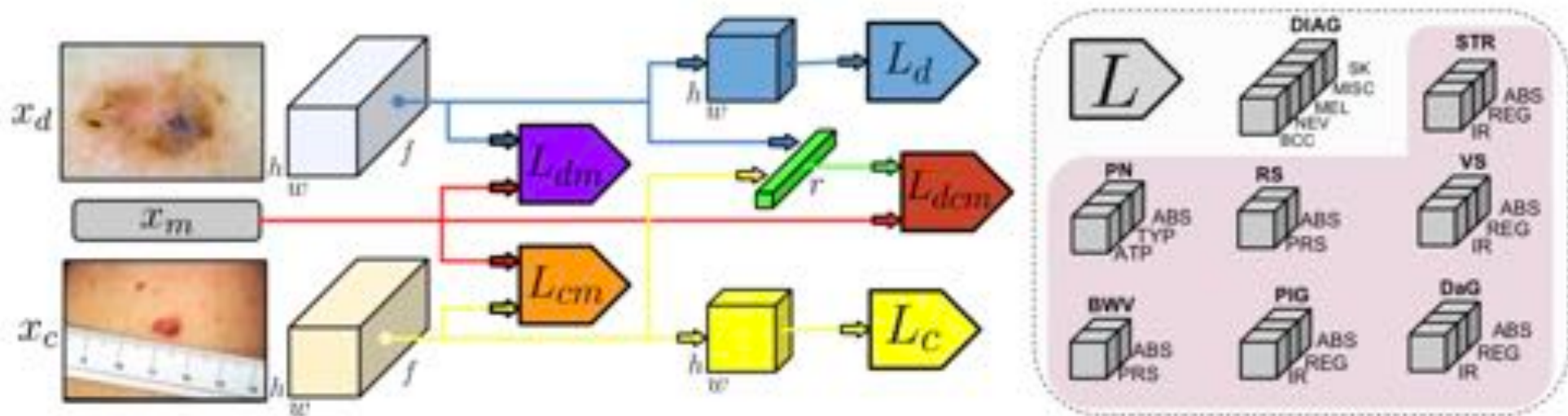
MEL

Multi-modal input

Clinical images
Dermoscopic images
Meta-data

$$L(x, y, z; \theta) = \ell(x, y; \theta) + \sum_{j=1}^7 \ell(x, z_j; \theta)$$

$$\begin{aligned}\mathcal{L}(x_d, x_c, x_m, y, z; \theta) &= L((x_d, x_c, x_m), y, z; \theta_{dcm}) \\ &+ L(x_d, y, z; \theta_d) + L((x_d, x_m), y, z; \theta_{dm}) \\ &+ L(x_c, y, z; \theta_c) + L((x_c, x_m), y, z; \theta_{cm})\end{aligned}$$



Multi-modal input



Lesion metadata
body location, roughness / elevation (flat, palpable, nodular)



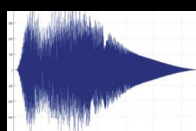
Patient data: age, gender, race, history



ARE NEURAL NETWORKS EFFECTIVE IN DETECTING MELANOMA USING GENOMIC DATA?

Abder-Rahman Ali,¹ Sally Jane O'Shea,^{2,3} Jingpeng Li,¹

1. Faculty of Natural Sciences, Computing Science and Mathematics, University of Stirling, UK.
2. Dermatology Department, Mater Private Hospital Cork, Ireland.
3. Faculty of Medicine, University College Cork, Ireland.



EBioMedicine

EBioMedicine 43 (2019) 107–113

Published by THE LANCET

Skin cancer detection by deep learning and sound analysis algorithms:
A prospective clinical study of an elementary dermatoscope

A. Dascalu ^{a,*}, E.O. David ^b

^a Department of Physiology and Pharmacology, Sackler School of Medicine, Tel Aviv University, Tel Aviv, Israel

^b Department of Computer Science, Bar-Ilan University, Ramat-Gan, Israel

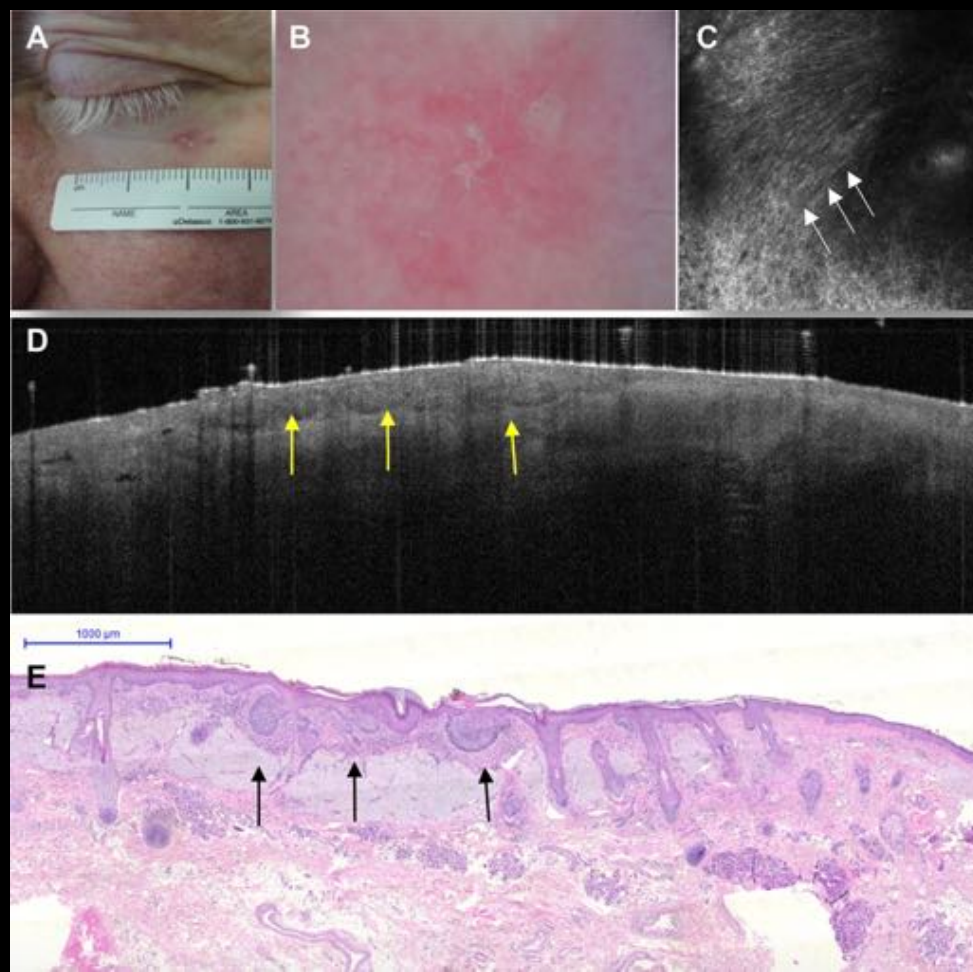
European Journal of Cancer 115 (2019) 79–83

Pathologist-level classification of histopathological melanoma images with deep neural networks



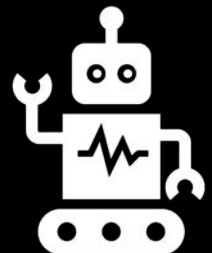
Achim Hekler ^a, Jochen Sven Utikal ^{b,c}, Alexander H. Enk ^d,
Carola Berking ^e, Joachim Klode ^f, Dirk Schadendorf ^f, Philipp Jansen ^f,
Cindy Franklin ^g, Tim Holland-Letz ^h, Dieter Krahl ⁱ, Christof von Kalle ^a,
Stefan Fröhling ^a, Titus Josef Brinker ^{a,d,*}

Clinical, dermoscopic, confocal microscopy, optical coherence tomography, histopathology



What's next?

- Disease classes: <10 → 1000s
- Datasets: 100s/1000s → millions of images
- Training: full-supervision → leveraging weak/no supervision
- Data sources: homogenous controlled → highly heterogenous sources
- Dimensions: 2D + static → real-world
- Modalities: unimodal → 3D + longitudinal/dynamic
- Deep modes: hand-crafted → multi-modal
- Beyond technical data-driven → automatic
- black-box → hybrid knowledge- & data-driven models
- susceptible → interpretable
- communities → resilient to adversarial attacks
- legal, ethical, societal, economic challenges → tighter computational-clinical collaboration



Thank you!

hamarneh@sfu.ca